P.S.D.C.-TR-15
SEPTEMBER 1, 1964

OFFICE OF
CIVIL DEFENSE

CORPS OF ENGINEERS
U.S. ARMY

TECHNICAL REPORT
THE BARRIER ATTENUATION INTRODUCED BY A VERTICAL WALL

PREPARED BY CONESCO
DIVISION OF FLOW CORPORATION
CAMBRIDGE MASSACHUSETTS

CONTRACT NO. DA-18-020-ENG-3096

PROTECTIVE STRUCTURES DEVELOPMENT CENTER
FORT BELVOIR, VIRGINIA

Protective Structures Development Center
M. M. Dembo, Acting Chief

Radiation Shielding Development Section
D. S. Reynolds, Jr., Acting Chief

This report covers a portion of the work authorized by Work Order No.: OCD-OS-63-148, 24 May 1963, Task No.: OCD 1117..

THE BARRIER ATTENUATION INTRODUCED BY A VERTICAL WALL

C. McDonnell, J. V. Velletri
A. W. Starbird, J. F. Batter

September 1, 1964

Prepared by Conesco Division of Flow Corporation

Contract DA-18-020-ENG-3096

Report to
Office of Civil Defense
from

Protective Structures Development Center
Joint Civil Defense Support Group
Office of Chief of Engineers/Bureau of Yards and Docks

ACKNOWLEDGEMENTS

The authors are indebted to Mr. Sheldon Hunt and Mr. D. S. Reynolds for their untiring efforts in the performance of the experiments described in this report and to Mr. C. Eisenhauer of the National Bureau of Standards for his suggestions and helpful criticisms.

ABSTRACT

A series of tests designed to evaluate the attenuation introduced by a vertical wall adjacent to a horizontal field of contamination is described. The variation of the resultant attenuation with height is found to agree well with theory. Actual attenuation values measured are higher than those theoretically predicted by an amount equivalent to approximately eight percent of the wall thickness.

TABLE OF CONTENTS

LIST OF ILLUSTRATIONS

LIST OF TABLES

CHAPTER 1

INTRODUCTION

With the establishment of the Radiation Test Facility at the Protective Structures Development Center, Ft. Belvoir, Virginia a series of continuing experiments has been initiated to evaluate the existing analytical methods employed in radiation shelter analysis work. These methods, which are based on theoretical infinite media computations, establish an engineering approach for determining the effectiveness of the shielding provided by structures and buildings against radioactive fallout resulting from a nuclear detonation. Detailed descriptions of the experimental equipment required, the experimental methods, and calibration measurements in these present programs are reported in "Description, Experimental Calibration, and Analysis of the Radiation Test Facility of the Protective Structures Development Center".[1]

In the analysis of structures[2, 3] with respect to the shielding afforded from radioactive fallout, the level of radiation at any point within the structure D is compared to that of a standard position D_o. For ease of computation D_o is usually taken as the dose rate three feet above an infinite, smooth plane, contaminated to the same density. The ratio D/D_o, called the reduction factor, is a measure of the effectiveness of that part of the structure against fallout radiation. This ratio in general terms is:

$$\frac{D}{D_o} = \left[\Sigma\, G(\omega)\right]\left[B(x_e, h)\right]$$

where the left bracketed term represents the attenuation due to geometric effects, and the right bracketed term represents the attenuation due to a barrier, as in a building wall. The barrier attenuation is a function of the mass thickness (x_e) of the barrier material, and the height above the ground plane of fallout contamination. It is this term, the barrier attenuation, introduced by a vertical wall to a horizontal plane of contamination, commonly called wall barrier factor, which is the subject of this series of experiments and of this report.

As the parameter of "wall barrier factor" is fundamental to all

reduction factor determinations whether analytical or experimental in nature, a series of experiments was devised to determine this parameter accurately for various building heights and wall mass thicknesses. The barrier factors determined from this group of experiments are used to check the barrier factors determined by analytical methods. In addition, they will be used in the detailed analysis of future experiments at this facility involving other building configurations.

The series of experiments found in this report extends the range over which the effects of the vertical barrier attenuation have been measured to a height of 33 feet and to a mass thickness of 150 psf. This range of mass thickness covers the majority of the values used in building construction in the United States.

CHAPTER 2

DESCRIPTION OF THE EXPERIMENT

The numerical information presented in the "Engineering Manual"[2], and its companion works,[3, 4], on barrier factors is derived from a theoretical analysis by Spencer.[5] Spencer's calculations of this parameter are based on a detector being immersed in a semi-infinite medium, exposed to a semi-infinite plane source and thus represents only one-half of the real situation. The attenuation calculated by Spencer, W(x, d) also include all back-scattered radiation.

This series of experiments attempted to duplicate physically the mathematical model of the analysis in that each detector was shielded to the rear to the extent necessary to duplicate the effect of a semi-infinite medium. The barrier factor of the Engineering Manual is numerically equal to twice Spencer's[5] function W(x, d) as the standard problem situation assumes an infinite rather than semi-infinite field of contamination. (See Figure 2.1). In the description of the various portions of the experimental work it is, however, easier to discuss the term W(x, d).

2.1 TEST STRUCTURE

The test structure at the Radiation Test Facility consists of a steel skeleton structure (Figure 2.2) of internal dimensions 24 by 36 feet, 36 feet high, with provisions for floors (or ceilings) at the 12, 24, and 36 foot elevations. The exterior building columns are 14B26 I beams which extend the height of the building. On the long dimension of the plan area there are ten such I beams giving nine wall-panel bays, while on the short side there are seven I beams giving six wall-panel bays. The clear distance between the web of each I beam column is approximately four feet.

The structure can be made up to represent a variety of building configurations by assembling the concrete panels (each 4 ft. by 4 ft. by 4 in. thick) into the required modular design. In the barrier-factor experiment only the walls were assembled; the longest (or southwest) wall facing the simulated contaminated field, was the only wall used for the experiment. The assembled structure is illustrated in Figure 2.3. Since each of the concrete panels was four inches thick, experiments were run

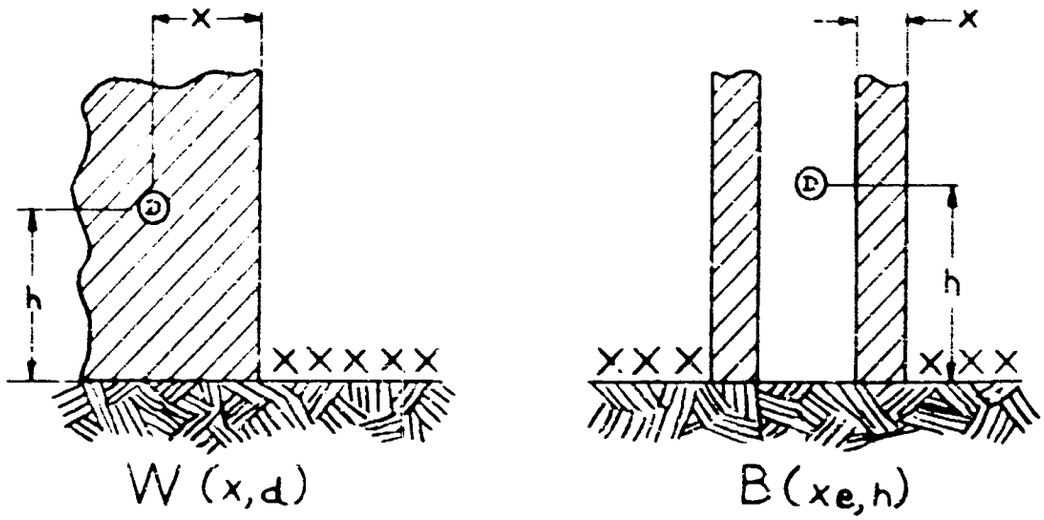

Figure 2.1 - Schematic Representation of Problem Geometry

in increments of four inches added wall thickness, thus providing walls of zero, four, eight and twelve inches total thickness. These wall thicknesses are equivalent to mass thicknesses of approximately 49 psf, 98 psf and 147 psf.

To reduce the amount of radiation penetrating the northwest wall which also partially faced the fallout field (this radiation would be extraneous to the experiment), the thickness of this wall was maintained at twelve inches for all barrier thicknesses. The remaining two walls, which are away from the field, were four inches thick for all experiments.

2.2 INSTRUMENTATION

Experimental data were obtained using either Victoreen Model 362, 200 mr, or Victoreen Model 239, 10 mr, non-direct reading ionization chambers (dosimeters) together with a Technical Operations Model 556 Charger Reader. Dosimeter selection was based upon the exposure time, the section of the field being simulated, the thickness

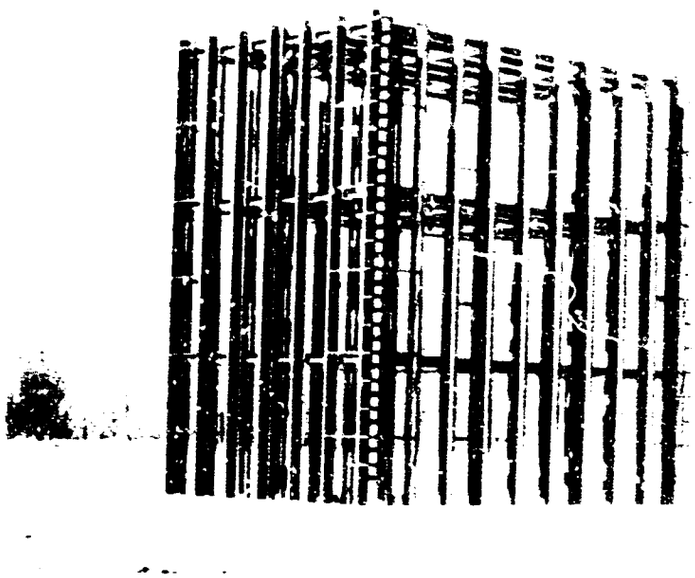

Figure 2.2 - Steel Skeleton of Test Structure

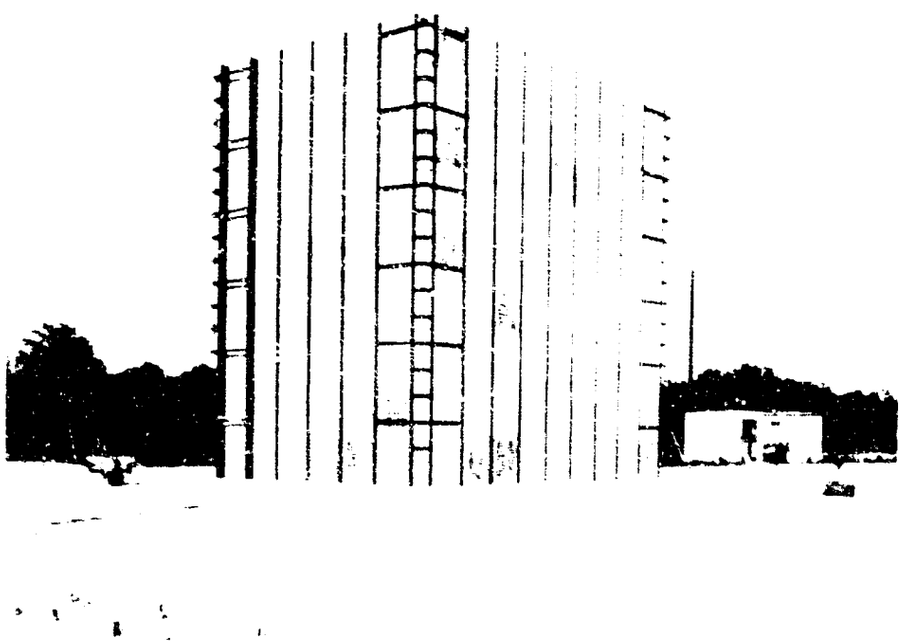

Figure 2.3 - Test Structure With All Walls in Place

of the wall, and the location of the dosimeters with respect to the contaminated area.

Prior to conducting the experiment, all dosimeters and the charger-reader were calibrated against a gamma source of known strength and Bureau of Standards calibrated Victoreen R meters. All of the dosimeters selected for use in the experiment responded to within + 2% to the known dose. The chambers were also checked at intervals during the experiment using a secondary calibration bench with a 100 millicurie source.

In this experiment, dosimeters were located inside and outside the test structure, against the barrier wall with the interior dosimeters located in the center of each of the nine 4 ft. panels that constitute the span of the side wall, at heights of 3.67, 6, 9.5, 14, 18, 21.5, 26, 30 and 33.3 feet above the datum plane. The three foot height was not used in this experiment since there is a recess in the panel at this elevation for attaching mounting hooks which can be used to lift and move the slab. These interior dosimeters were taped directly to the concrete wall in a horizontal position, and shielded on all the remaining sides with concrete block. The purpose of this shielding was to insure that the total effect of backscattered radiation was included in the measurement in order that direct comparisons could be made with existing theoretical calculation. This shielding (Figure 2.4 and Figure 2.5) consisted of 4 inch by 8 inch by 16 inch solid concrete blocks which were placed about and to the rear of every dosimeter. The units of block shielding were supported by a system of wooden frame shelving (Figure 2.6).

Data for walls of zero mass thickness were obtained by placing dosimeters on the exterior surface of the wall at the same elevations as the interior dosimeters (Figure 2.7) with the dosimeters mounted against the concrete wall so that all the backscattered radiation would be present. Consideration was given to the thickness of the wall for this experiment. An eight-inch wall provided the required thickness (equivalent to about three mean free paths) necessary to obtain essentially 100 percent of the infinite medium backscattered radiation. However, if an eight inch wall were used, the vertical steel beams would have projected beyond the wall face thereby introducing some shadowing of the field as viewed by the detector. Because of the practical problems in the assembly of the wall of the building, a four or eight inch thick wall is recessed back from the outside flange of the vertical I beams. A dosimeter located on

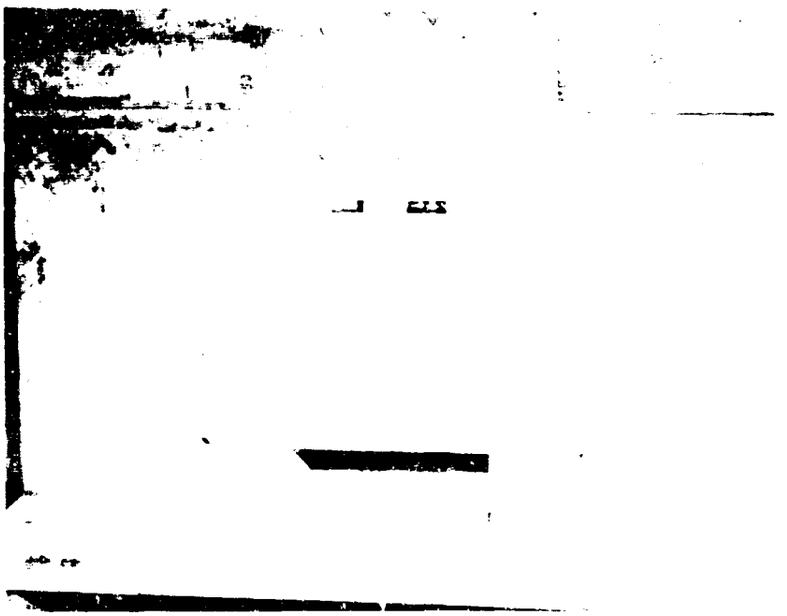

Figure 2.4 - Dosimeter in Place
Unshielded

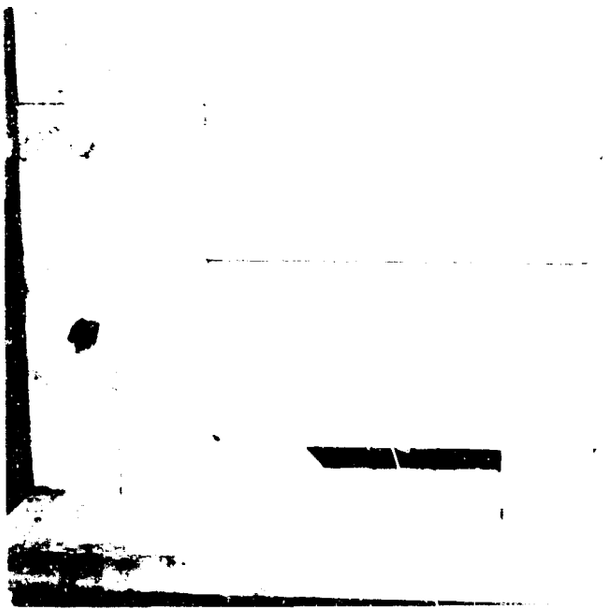

Figure 2.5 - Dosimeter Shielded

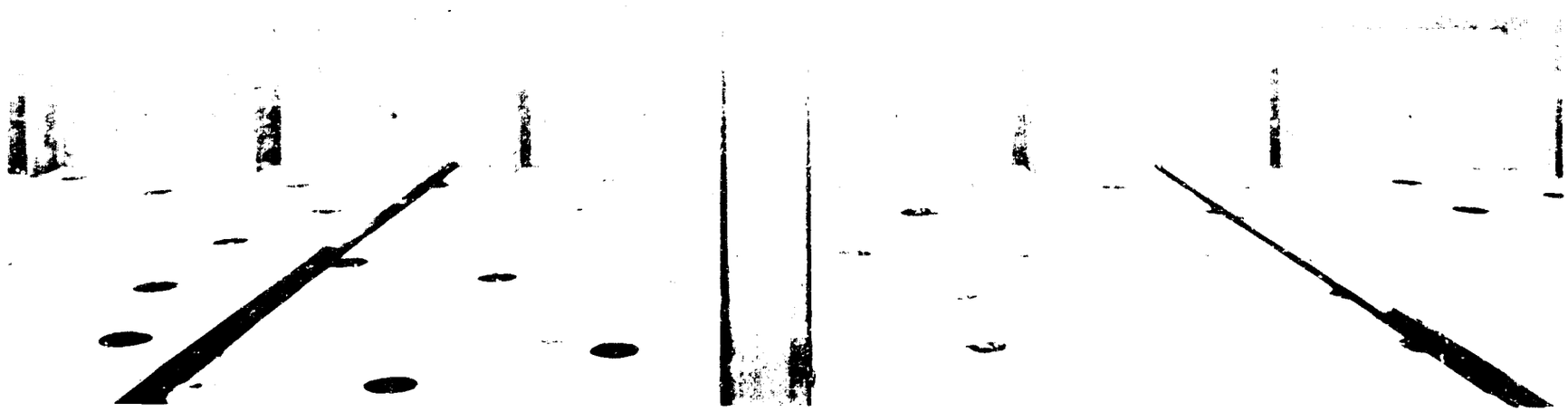

Figure 2.6 - Interior View illustrating Support of Dosimeter Shielding

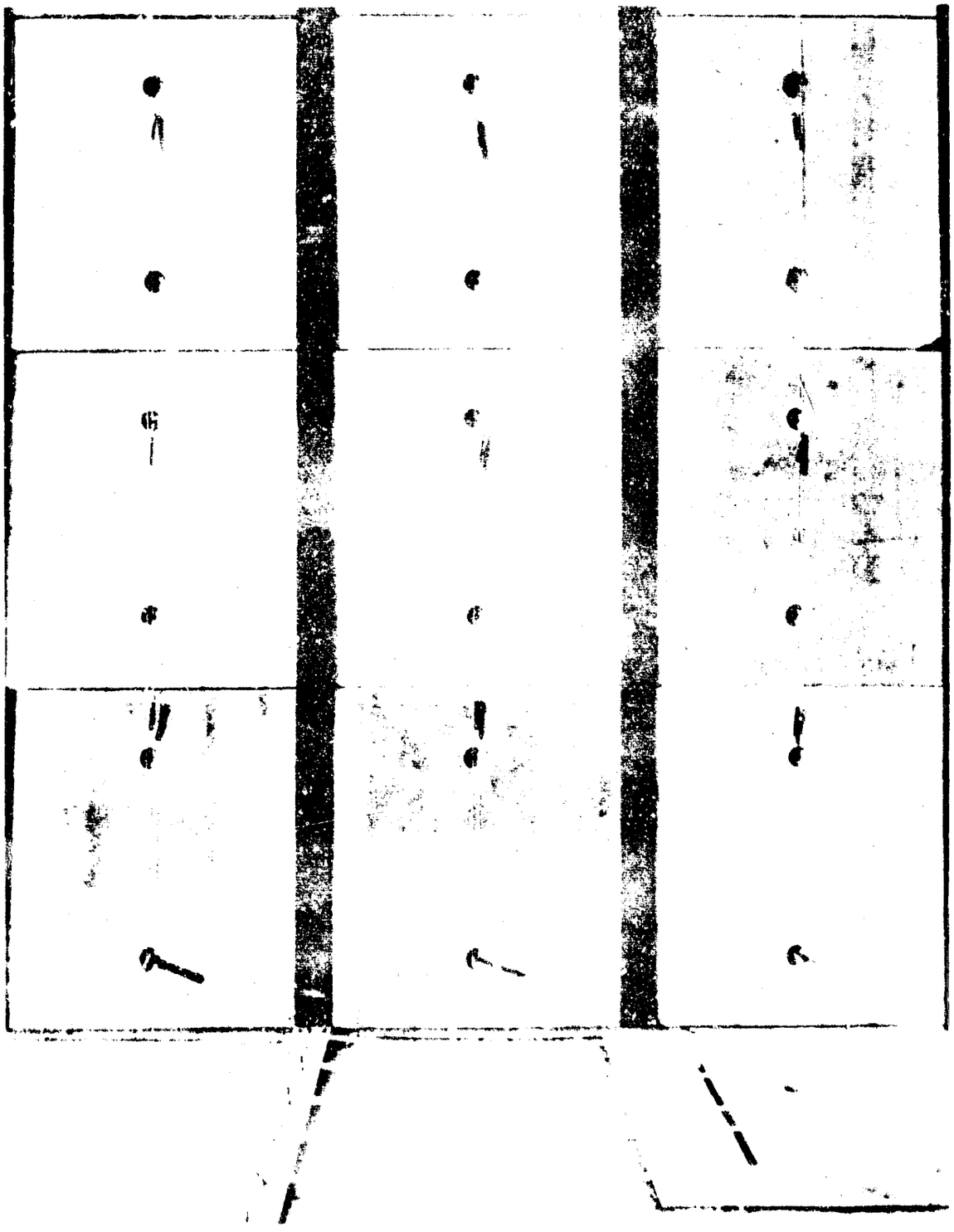

Figure 2.7 - Exterior View Illustrating Placement of Detectors for the Case of Zero Thickness

the center of a panel between the I beams will see a shadow sector presented by the outer flange of the I beam (Figure 2.8). With a full twelve inch wall, the exterior surface of the panels are flush with the outer flange of the I beam, eliminating the sector shadow of the outer flange (Figure 2.9). For these reasons data were taken for the case of zero mass thickness using the twelve inch concrete wall as the back-scattering element.

2.3 SIMULATED FIELD

The simulated fallout field at the test site was initially planned and laid out with the intent that it be a semi-permanent part of the test facility, used for a large number of experiments. The field (the design of which is described in detail in Reference 1) consists of a quadrant of a circle of 452 ft. radius, concentric with the test structure, which is divided into four annular test areas (See Figure 2.10). By using this existing field for the series of barrier factor experiments the center of the field was not located at the center of the barrier wall, but rather was displaced 13-1/3 feet to the center of the structure (Figure 2.11). This displacement creates no significant effect on the experiment as the detector positions were shielded by a minimum of 20 inches of concrete (12 inches in the building wall, 8 inches in the form of 4 x 8 x 16" blocks stacked behind the detector) from the extraneous portion of the test field*. Since only one wall of the structure was involved in the experiment, the simulated field was actually of half symmetry for this case.

The simulated field consists of four annular areas, each of approximately equal contribution of radiation dosage to the standard reference position. A contaminated field is simulated by pumping sealed radioisotopic sources at constant velocity through a network of tubing that occupies each of the four annular areas. Only one source is pumped in a selected area at one time. The infinite field dose is thus the sum of the desage received by the detector from each of the four areas plus an estimated contribution based on the outermost simulated area to represent far field sources of contamination.

*That portion of the field lying behind the horizontal line created by the intersection of the wall and the datum plane.

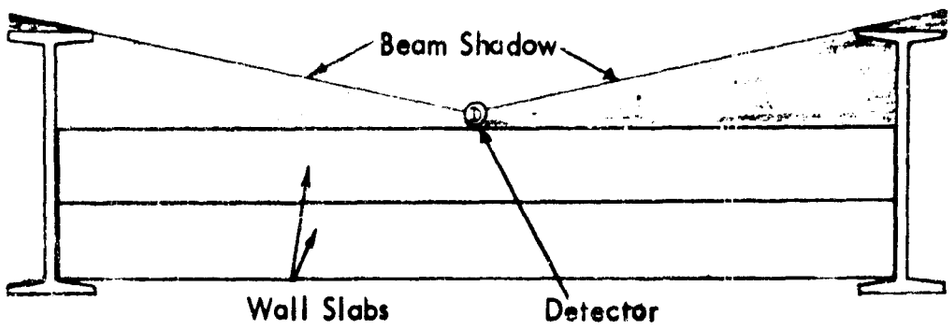

Figure 2.8 - Dosimeter Shadow With an Eight Inch Thick Wall

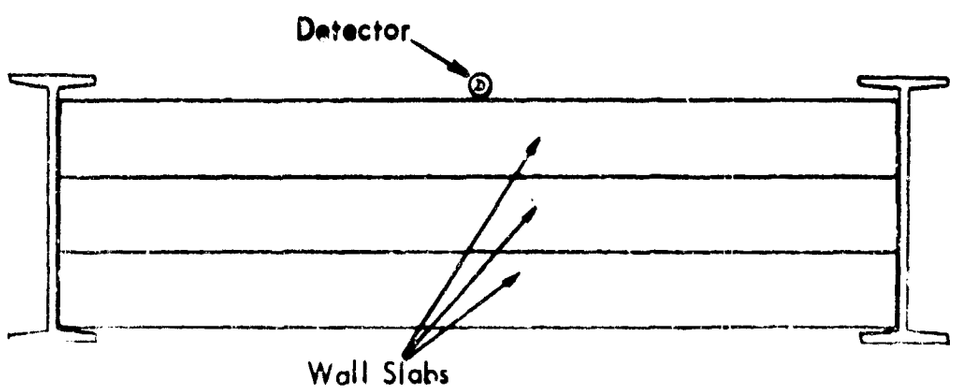

Figure 2.9 - Exterior Dosimeter Placement with a Twelve Inch Wall

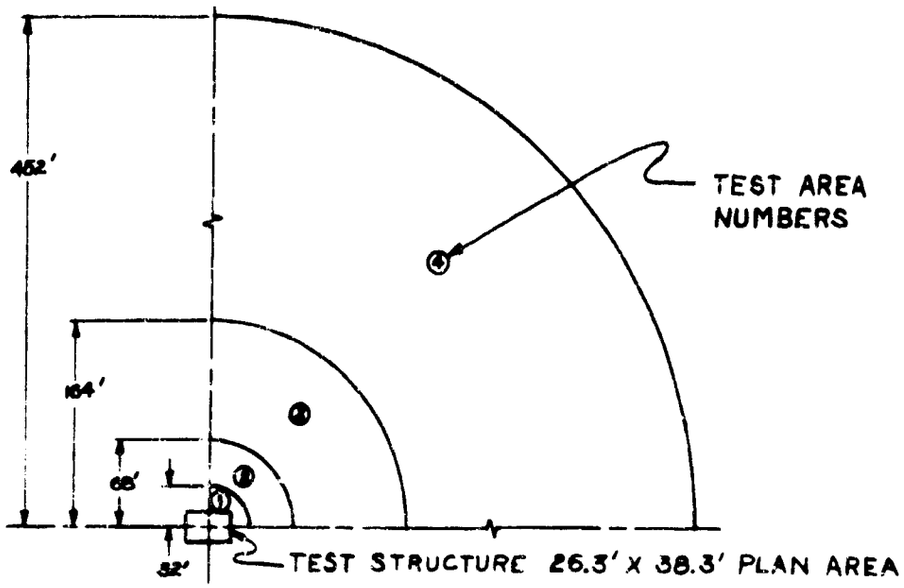

Figure 2.10 - Plan View of the Test Area

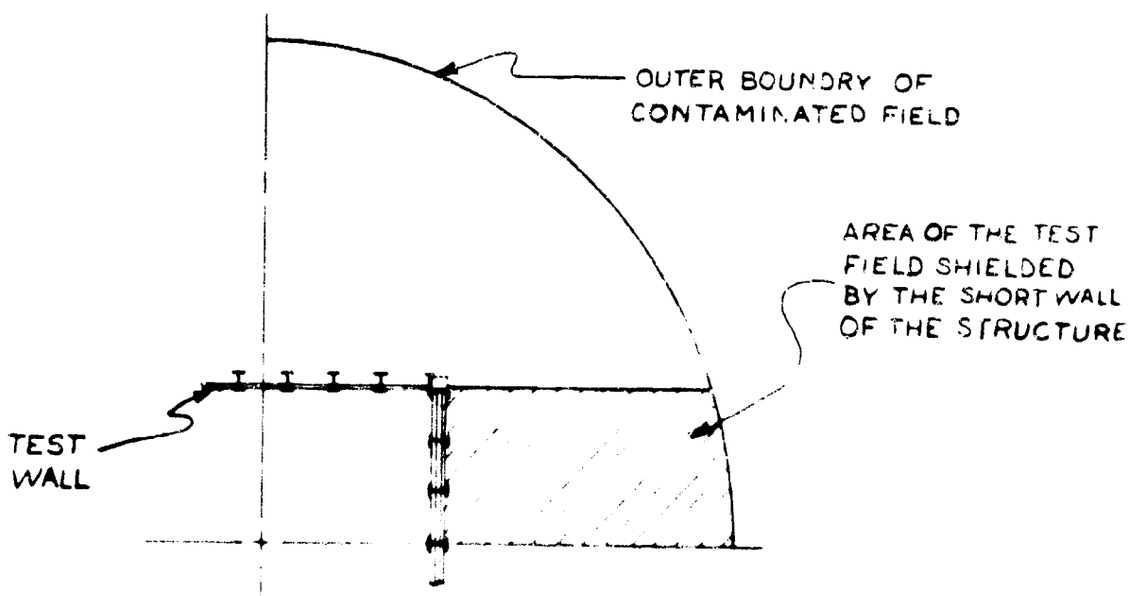

Figure 2.11 - Placement of the Test Wall Relative to the Test Field

2.4 EQUIPMENT

Throughout the entire series of experiments planned at the Radiation Test Facility, the equipment used is basic and common to all experiments. It consists of a pump system, source storage container, a sealed source, and a system of polyethylene tubing. As previously described, the sealed source is pumped from its container through the tubing surrounding the test structure and back to the storage container thus completing an exposure. A brief description of the test equipment required for this operation is presented here. The reader is, however, referred to Reference 1 for a more complete description including methods of operation and operational characteristics.

The pump unit consists of four positive displacement, proportioning pumps, mechanically linked to a drive mechanism such that their displacement positions are staggered by 90 degrees to reduce pulsing flow. The volume output of the pumps and hence the velocity of the liquid, and source assembly in the tubing, may be varied either by adjustment of a variable speed drive or by alteration of the pump stroke.

The tubing through which the source travels is made of polyethylene with an additive to reduce damage from constant exposure to sunlight. This tubing has dimensions of 0.625 inches O. D. and 0.375 inches I. D. Special stainless fittings that join sections of tubing without altering its inner diameter are employed to connect the tubing to other lengths of tubing or to the storage container.

The source storage container consists of a lead filled steel shell mounted on solid rubber tires so that it is easily movable with the use of a skid spotter. Two pairs of 3/8" I. D. stainless steel tubes, which house the source assemblies, pass through the container near its center. The source assembly is retained in the container by a safety clamp device. The output of the pump and one end of the tubing representing the test field are connected to the tube of the storage container, containing the source, while the return tubing from the field and the pump suction tubing are connected to the appropriate empty storage tube which will receive the returning source. Operation is then achieved by releasing the safety clamp on the source assembly and diverting the output of the pumping system to the test loop. A schematic diagram of the system is presented in Figure 2.12

The sealed sources employed in this experiment are nominally

described as 6, 60, and 600 curies of Cobalt-60. These assemblies each consist of an encapsulated Co-60 source attached to a hydraulic piston by means of a flexible cable. The piston leads the source so that hydraulic pressure on the cable side of the piston will force the piston through the tubing.

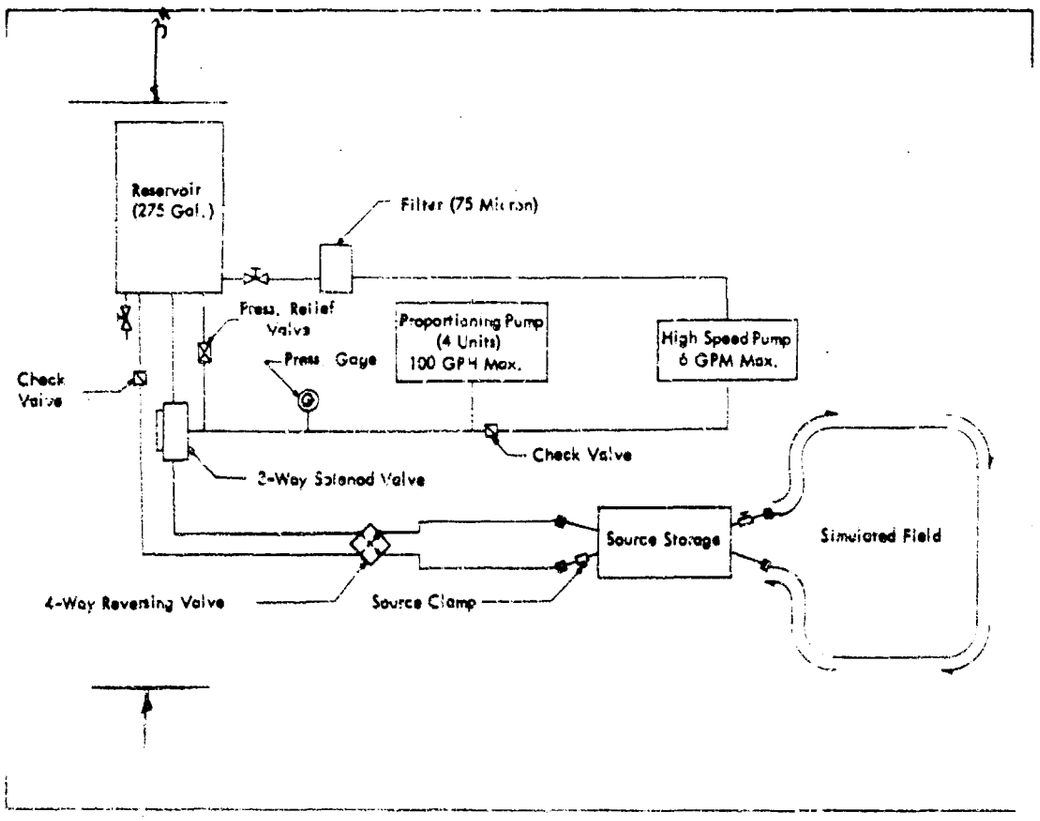

Figure 2.12 - Schematic Diagram of the Source Circulation System

The calibration methods, which represent an inter-calibration with a National Bureau of Standards calibrated Victoreen R meter, are described in detail in Reference 1. The source strengths from this calibration, based upon the specific irradiance of 14.0 RHF, corrected for time decay to July 1, 1964 are:

Source No. 1	516 Curies
Source No. 2	50.4 Curies
Source No. 3	5.04 Curies

CHAPTER 3

DESCRIPTION OF EXPERIMENTAL DATA

The experiment consisted of four phases, one for each of the nominal wall thicknesses of 0, 49, 98, 147 psf. Detectors were located at various heights from 3.67 ft. to 33.3 ft. and were placed in a manner such that the data obtained, could be compared directly with that obtained from theory.

3.1 REPRODUCIBILITY AND ACCURACY OF EXPERIMENTAL DATA

The accuracy of the data obtained is related to the standard deviation of both the detector response, and the determination of the mass thickness of the panels that constitute the barrier wall. The detectors, together with the charger-reader were calibrated and grouped into a lot that gave a response range of ±2 percent to a known source strength. As indicated in Reference 1, these detectors in two previous experimental test series undertaken under a wide variety of atmospheric conditions, source sizes and exposure times, were found to have a standard deviation of reproducibility of approximately 2.3%. The standard deviation of experimental error related to the instrument readings, source strengths and exposure conditions is thus approximately 3%

Twenty-three of the concrete wall panels used to construct the test wall were selected at random and were measured and weighed to establish their mass thickness. Dimensionally, the panels varied by about ± 1/16th inch from the basic dimensions, introducing an uncertainty of approximately ± 1/4 percent. The panels were weighed using a Baldwin load cell calibrated to one part in a thousand against a known mass of water. Each slab was weighed in turn producing weights varying from 755 lbs. to 780 lbs. The average slab weight was determined as 767 lbs. with a standard deviation of 8 pounds, (Figure 3.1). Expressed in terms of mass thickness this represented a mass thickness of 49 psf with a standard deviation of 0.5 psf..

A more detailed description of error analysis is presented as Appendix A.

3.2 NORMALIZATION OF DATA

All dosimeter readings obtained from the experimental runs

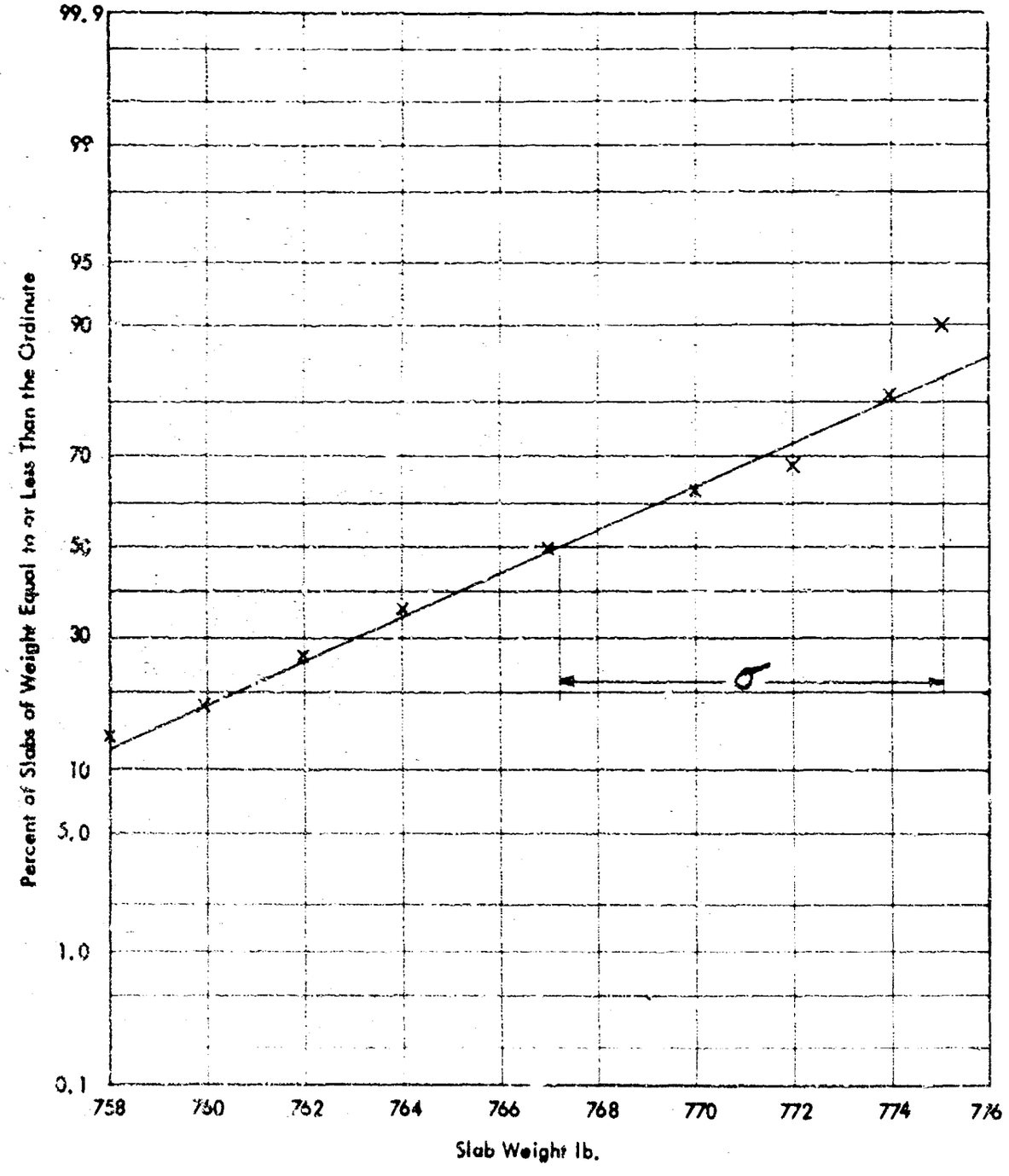

Figure 3.1 - Statistical Analysis of Slab Weight

were normalized to a "per hour basis" for an equivalent contamination density of one curie of Cobalt-60 per square foot. This is the source density required to produce a radiation field of 464 R/hr at the three foot height above an infinite, smooth, uniformly-contaminated plane.[1] Due to the large number of dosimeter readings taken, data normalization was programmed for an RCA 301 computer. In this program dosimeter readings are converted to an R/hr basis using dosimeter calibration constants, exposure time, source strength, and the atmospheric temperature-pressure corrections. The equation used to correct readings of roentgens to a standard curie per square foot basis is:

$$I_o = \frac{DA}{tS_o}$$

where

I_o = the normalized data in (R/hr)/(curie/ft^2)

D = measured dose normalized to standard conditions

A = area of the contaminated field (ft^2)

S_o = source strength (curies)

t = exposure time (hours)

3.3 DESCRIPTION OF TEST DATA

As described in the preceding chapter, dosimeters were located at elevations of 3.67, 6, 9.5, 14, 18, 21.5, 26, 30 and 33.3 feet on the outside test structure wall for the case of x = 0 psf, and on inside of this wall for the cases of nominal thicknesses of 49, 98, and 147 psf. The wall, which consisted of nine vertical four foot panel bays, faced a simulated fallout field that represented half symmetry geometry for the case of the wall only.

As only half of the total field was contaminated the mathematical technique of summing mirror images was employed to account for that half of the test area not directly simulated. Thus to obtain the values of the radiation emerging through the wall, it is necessary, for a

given elevation, to add the values of the first and ninth position (-16 and + 16 foot horizontal distance in the following tables, (see Figure 3.2) the second and eighth position, Table 3.1 is a tabulation of the horizontal dosimeter position, etc., while the value at the center position was doubled. All experimental data are normalized to roentgens per hour for a source density of one curie per square foot and are presented in tabular form in Tables 3.2 through 3.3 grouped by mass thickness as follows:

TABLE 3.2 contains data for mass thickness X = 0 psf
TABLE 3.3 contains data for mass thickness X = 49 psf
TABLE 3.4 contains data for mass thickness X = 98 psf
TABLE 3.5 contains data for mass thickness X = 147 psf

All data are in terms of specific dose rate which is in units of roentgen per hour per curie per square foot of field area.

The test areas referred to in these tables are those of Figure 2.10.

TABLE 3.1

Horizontal Dosimeter Positions

Dosimeter	Distance From Center of Wall
A	+ 16 ft
B	∓ 12
C	∓ 8
D	∓ 4
E	0

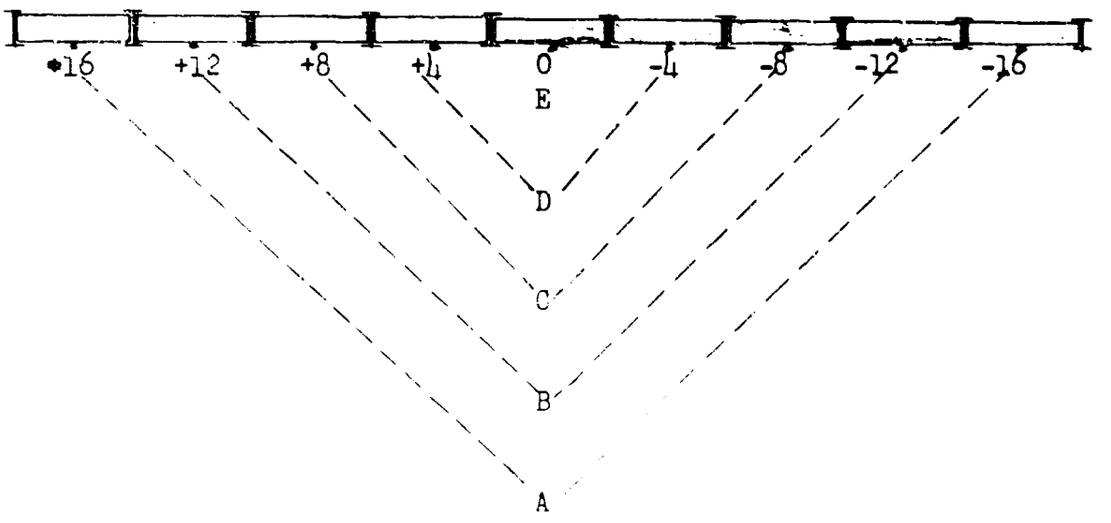

Figure 3.2 - Plan View of Dosimeter Locations Along Experimental Wall

TABLE 3.2

DOSE RATES FOR 0 PSF BARRIER

(R/HR NORMALIZED TO A SOURCE DENSITY OF 1 CURIE/SQ. FT.)

AREA 1 (HALF SYMMETRY)

HEIGHT	HORIZONTAL DISTANCE FROM CENTER OF BARRIER (FT.)								
(FT.)	-16	-12	-8	-4	0	+4	+8	+12	+16
3.0	80.2	79.0	79.6	70.6	49.7	26.7	14.7	9.89	6.04
3.67	73.0	73.6	70.6	63.4	46.7	25.1	15.0	9.73	6.30
6.0	51.5	52.1	50.3	45.5	33.5	22.0	14.3	10.1	6.42
9.5	33.1	33.1	32.5	29.4	23.4	17.7	12.7	9.08	6.48
14.0	19.9	20.9	19.9	18.0	16.1	13.1	10.5	7.24	5.84
18.0	14.0	14.4	14.1	13.6	12.2	10.1	8.04	6.13	5.14
21.5	11.0	11.0	10.8	9.99	9.21	7.18	6.60	5.25	4.55
26.0	7.24	7.00	7.12	6.65	6.42	5.49	5.08	4.79	3.85
30.0	5.90	5.72	5.43	5.25	4.85	4.67	4.44	3.68	3.21
33.3	4.55	4.44	4.55	4.44	4.26	3.91	3.62	3.33	3.04

AREA 2 (HALF SYMMETRY)

3.0	43.8	38.0	31.5	27.4	24.3	20.5	17.1	15.5	13.2
3.67	43.6	36.2	32.4	28.1	24.1	21.4	17.9	15.2	13.2
6.0	43.6	35.6	32.1	27.7	24.1	20.6	18.0	15.2	14.2
9.5	38.6	34.7	31.2	27.6	23.4	19.4	17.3	15.2	13.6
14.0	34.7	30.3	27.7	25.3	22.1	19.1	16.5	14.7	13.2
18.0	30.0	26.5	25.0	22.4	20.2	17.1	15.2	14.2	12.9
21.5	25.9	24.1	23.0	20.6	18.2	16.1	14.5	13.7	11.9
26.0	23.0	20.6	20.6	17.9	16.4	14.8	13.7	12.4	11.6
30.0	20.6	18.2	17.7	16.0	14.6	13.2	12.1	11.1	10.1
33.3	18.5	16.0	16.0	14.2	13.8	12.2	11.1	10.6	9.56

TABLE: 3.2

DOSE RATES FOR 0 PSF BARRIER

(R/HR NORMALIZED TO A SOURCE DENSITY OF 1 CURIE/SQ. FT.)

AREA 3 (HALF SYMMETRY)

HEIGHT	HORIZONTAL DISTANCE FROM CENTER OF BARRIER (FT.)								
(FT.)	-16	-12	-8	-4	0	+4	+8	+12	+16
3.0	26.7	24.6	23.7	23.1	20.3	19.4	18.5	[illegible]	16.3
3.67	27.8	26.0	23.6	23.4	21.8	20.7	19.3	18.9	17.9
6.0	28.3	26.4	24.8	23.3	22.5	21.4	19.8	18.2	17.9
9.5	28.8	26.9	25.0	24.1	22.9	21.0	20.8	18.9	18.6
14.0	28.8	27.4	25.0	24.8	23.1	22.4	21.7	18.9	18.4
18.0	28.6	26.9	26.0	23.9	22.8	21.6	19.8	19.3	18.2
21.5	28.6	26.0	25.0	23.9	22.7	21.7	20.8	18.9	18.4
26.0	27.4	26.0	24.5	23.1	22.7	19.5	19.8	18.2	18.2
30.0	26.9	25.5	24.3	23.1	21.8	20.6	19.8	18.9	17.9
33.3	26.0	23.6	24.1	22.2	20.6	20.6	19.3	17.9	18.4

AREA 4 (HALF SYMMETRY)

3.0	16.7	16.1	16.0	15.5	14.4	14.9	14.3	14.1	13.7
3.67	18.1	17.4	17.1	16.3	16.0	15.8	15.6	14.8	14.8
6.0	19.4	18.7	18.7	17.6	17.4	16.6	17.1	16.4	16.4
9.5	21.0	19.9	19.4	19.2	18.4	18.3	17.9	17.4	17.1
14.0	21.5	20.3	20.4	19.1	19.2	19.1	18.7	18.4	18.1
18.0	22.3	20.5	20.9	19.9	19.6	19.2	18.7	18.4	18.4
21.5	22.3	20.9	20.4	19.7	19.4	19.2	19.5	18.7	18.4
26.0	22.5	20.9	20.7	20.0	19.7	19.6	18.7	18.7	18.4
30.0	22.5	21.3	20.9	20.4	19.9	19.8	18.7	18.9	18.4
33.3	22.7	21.8	20.7	20.2	19.9	19.7	19.0	18.7	18.7

TABLE 3.3

DOSE RATE FOR 49 PSF BARRIER

(R/HR NORMALIZED TO A SOURCE DENSITY OF 1 CURIE/SQ. FT.)

AREA 1 (HALF SYMMETRY)

HEIGHT	HORIZONTAL DISTANCE FROM CENTER OF BARRIER (FT.)								
(FT.)	-16	-12	-8	-4	0	+4	+8	+12	+16
3.67	14.0	15.2	14.0	12.2	9.83	4.21	2.30	1.12	.584
6.0	7.96	8.90	9.13	7.72	5.27	3.01	1.67	1.01	.519
9.5	4.68	5.03	5.15	4.45	3.33	2.30	1.47	.812	.479
14.0	2.37	2.82	2.62	2.30	1.92	1.32	.913	.597	.345
18.0	1.27	1.52	1.47	1.34	1.09	.753	.595	.393	.247
21.5	.746	.866	.834	.828	.726	.524	.405	.300	.190
26.0	.429	.536	.464	.417	.418	.333	.245	.201	.140
30.0	.303	.333	.319	.302	.286	.247	.181	.154	.110
33.3	.243	.247	.220	.231	.192	.165	.148	.104	.0934

AREA 2 (HALF SYMMETRY)

3.67	13.1	11.3	8.89	7.26	6.99	5.17	4.39	3.70	2.88
6.0	11.9	10.0	8.80	7.27	5.87	4.80	4.25	3.50	2.61
9.5	9.72	8.94	7.82	6.99	5.73	5.08	4.39	3.43	2.74
14.0	7.60	7.55	6.85	6.15	5.01	4.39	3.57	3.22	2.47
18.0	6.57	6.36	5.17	4.87	4.32	3.57	3.29	2.67	2.26
21.5	5.08	5.18	4.56	4.12	3.70	2.95	2.88	2.40	1.85
26.0	4.32	3.98	3.50	3.09	3.02	2.67	2.06	1.90	1.60
30.0	3.02	3.22	3.02	2.74	2.47	2.19	1.90	1.70	1.26
33.3	3.22	3.02	2.47	2.24	2.04	1.94	1.84	1.43	1.33

TABLE: 3.3

DOSE RATE FOR 49 PSF BARRIER

(R/HR NORMALIZED TO A SOURCE DENSITY OF 1 CURIE/SQ. FT.)

AREA 3 (HALF SYMMETRY)

HEIGHT	HORIZONTAL DISTANCE FROM CENTER OF BARRIER (FT.)								
(FT.)	-16	-12	-8	-4	0	+4	+8	+12	+16
3.67	7.37	7.37	6.29	5.89	6.19	5.21	5.01	4.72	4.22
6.0	8.01	7.43	7.02	6.29	5.50	5.30	5.06	5.11	4.22
9.5	7.91	7.32	6.83	6.43	5.89	5.70	5.60	4.91	4.42
14.0	7.52	7.37	7.07	6.43	5.89	5.60	5.30	4.96	4.32
18.0	7.56	7.17	6.63	5.99	5.89	5.21	5.21	4.62	4.52
21.5	7.02	6.83	6.43	6.09	5.60	5.01	5.11	4.62	4.13
26.0	7.17	6.53	5.89	5.40	5.50	5.11	4.81	4.37	4.08
30.0	6.68	6.29	5.89	5.60	5.35	5.11	4.62	4.32	3.93
33.3	6.63	6.43	5.70	5.21	5.30	4.72	4.72	4.13	4.13

AREA 4 (HALF SYMMETRY)

3.67	4.51	4.42	3.96	3.77	4.19	3.59	3.59	3.59	3.40
6.0	4.60	4.69	4.51	4.42	4.05	4.05	3.96	4.14	3.77
9.5	5.15	4.97	4.78	4.69	4.42	4.51	4.69	4.23	4.05
14.0	5.15	5.24	5.15	5.06	4.78	4.60	4.60	4.42	4.14
18.0	5.70	5.43	5.06	4.78	4.88	4.42	4.69	4.32	4.32
21.5	5.67	5.43	5.06	4.78	4.78	4.51	4.55	4.51	3.77
26.0	5.52	5.34	4.97	4.69	4.88	4.69	4.51	4.51	4.14
30.0	5.52	5.24	5.24	4.97	4.88	4.78	4.60	4.42	4.32
33.3	5.89	5.52	5.01	4.97	4.97	4.83	4.78	4.42	4.60

TABLE: 3.4

DOSE RATE FOR 98 PSF BARRIER

(R/HR NORMALIZED TO A SOURCE DENSITY OF 1 CURIE/SQ. FT.)

AREA 1 (HALF SYMMETRY)

HEIGHT	HORIZONTAL DISTANCE FROM CENTER OF BARRIER (FT.)								
(FT.)	-16	-12	-8	-4	0	+4	+8	+12	+16
3.67	4.11	4.43	4.19	3.87	2.64	1.04	.495	.225	.112
6.0	2.21	2.58	2.41	2.07	1.39	.716	.348	.210	.101
9.5	1.12	1.21	1.18	1.12	.781	.494	.307	.167	.0899
14.0	.466	.513	.511	.448	.375	.262	.167	.109	.0605
18.0	.233	.276	.254	.234	.206	.142	.103	.0701	.0440
21.5	.130	.150	.148	.153	.123	.0911	.0729	.0509	.0350
26.0	.0745	.0818	.0784	.0708	.0708	.0536	.0400	.0307	.0231
30.0	.0440	.0478	.0481	.0485	.0435	.0364	.0286	.0247	.0157
33.3	.0350	.0372	.0322	.0311	.0286	.0250	.0218	.0175	.0157

AREA 2 (HALF SYMMETRY)

3.67	4.23	3.68	2.82	2.47	2.18	1.59	1.52	1.03	.771
6.0	3.61	3.29	2.51	2.16	1.80	1.44	1.13	.977	.694
9.5	3.14	2.82	2.39	2.02	1.68	1.41	1.23	.925	.771
14.0	2.09	2.09	1.93	1.62	1.44	1.21	.977	.797	.610
18.0	1.76	1.64	1.46	1.28	1.21	.925	.796	.676	.557
21.5	1.39	1.39	1.26	1.18	.977	.822	.690	.557	.451
26.0	1.03	1.00	.899	.796	.756	.584	.530	.451	.332
30.0	.771	.782	.716	.690	.610	.517	.424	.385	.292
33.3	.769	.703	.610	.583	.530	.451	.424	.345	.318

TABLE: 3.4

DOSE RATE FOR 98 PSF BARRIER

(R/HR NORMALIZED TO A SOURCE DENSITY OF 1 CURIE/SQ. FT.)

AREA 3 (HALF SYMMETRY)

HEIGHT	HORIZONTAL DISTANCE FROM CENTER OF BARRIER (FT.)								
(FT.)	-16	-12	-8	-4	0	+4	+8	+12	+16
3.67	2.44	2.16	2.06	1.85	1.85	1.61	1.55	1.41	1.21
6.0	2.51	2.58	2.06	1.92	1.65	1.55	1.41	1.44	1.17
9.5	2.35	2.13	2.80	1.92	1.72	1.61	1.68	1.48	1.37
14.0	2.16	2.20	1.99	1.89	1.79	1.58	1.61	1.48	1.30
18.0	2.32	2.16	1.89	1.85	1.75	1.55	1.51	1.37	1.30
21.5	2.09	2.09	1.79	1.82	1.58	1.44	1.37	1.30	1.17
26.0	2.13	1.82	1.79	1.61	1.61	1.44	1.37	1.20	.996
30.0	1.89	1.85	1.75	1.72	1.58	1.30	1.27	1.17	.996
33.3	2.13	1.85	1.65	1.55	1.51	1.37	1.30	1.20	1.20

AREA 4 (HALF SYMMETRY)

3.67	1.21	1.23	1.08	1.07	1.15	.993	1.02	.986	.978
6.0	1.42	1.36	1.29	1.26	1.14	1.06	1.05	1.09	1.04
9.5	1.47	1.42	1.34	1.35	1.27	1.25	1.31	1.20	1.19
14.0	1.48	1.44	1.43	1.36	1.35	1.29	1.22	1.26	1.17
18.0	1.66	1.55	1.50	1.38	1.38	1.28	1.28	1.24	1.22
21.5	1.51	1.50	1.38	1.44	1.28	1.24	1.29	1.20	1.16
26.0	1.60	1.48	1.47	1.38	1.35	1.30	1.30	1.25	1.14
30.0	1.63	1.51	1.47	1.46	1.46	1.33	1.28	1.22	1.18
33.3	1.69	1.54	1.43	1.43	1.38	1.34	1.38	1.26	1.26

TABLE: 3.5

DOSE RATE FOR 147 PSF BARRIER

(R/HR NORMALIZED TO A SOURCE DENSITY OF 1 CURIE/SQ. FT.)

AREA 1 (HALF SYMMETRY)

HEIGHT	HORIZONTAL DISTANCE FROM CENTER OF BARRIER (FT.)								
(FT.)	-16	-12	-8	-4	0	+4	+8	+12	+16
3.67	1.13	1.25	1.11	1.01	.684	.273	.105	.0435	.0227
6.0	.528	.584	.568	.500	.321	.164	.0708	.0416	.0199
9.5	.238	.276	.284	.253	.187	.102	.0575	.0310	.0179
14.0	.0834	.101	.105	.0890	.0742	.0519	.0305	.0201	.0113
18.0	.0437	.0486	.0482	.0447	.0393	.0254	.0193	.0135	.00856
21.5	.0229	.0270	.0260	.0254	.0202	.0164	.0132	.00911	.00698
26.0	.0105	.0134	.0141	.0126	.0132	.0109	.00765	.00661	.00479
30.0	.00608	.00765	.00856	.00644	.00814	.00721	.00526	.00506	.00357
33.3	.00540	.00514	.00559	.00584	.00573	.00551	.00445	.00412	.00374

AREA 2 (HALF SYMMETRY)

3.67	1.27	1.05	.890	.731	.600	.465	.349	.246	.200
6.0	1.15	.937	.784	.627	.470	.387	.295	.257	.172
9.5	.883	.732	.663	.571	.460	.373	.325	.233	.183
14.0	.600	.552	.508	.426	.365	.312	.235	.197	.139
18.0	.513	.445	.378	.334	.295	.226	.200	.158	.122
21.5	.387	.365	.319	.286	.250	.194	.178	.131	.112
26.0	.231	.243	.219	.190	.181	.147	.123	.109	.0877
30.0	.171	.173	.179	.148	.135	.120	.100	.0877	.0668
33.3	.183	.162	.133	.133	.122	.111	.0920	.0791	.0744

TABLE: 3.5

DOSE RATE FOR 147 PSF BARRIER

(R/HR, NORMALIZED TO A SOURCE DENSITY OF 1 CURIE/SQ. FT.)

AREA 3 (HALF SYMMETRY)

HEIGHT	HORIZONTAL DISTANCE FROM CENTER OF BARRIER (FT.)								
(FT.)	-16	-12	-8	-4	0	+4	+8	+12	+16
3.67	.728	.642	.543	.523	.526	.450	.419	.370	.346
6.0	.710	.619	.560	.516	.440	.409	.375	.380	.319
9.5	.672	.611	.570	.526	.478	.441	.429	.375	.356
14.0	.636	.599	.575	.521	.480	.450	.399	.372	.322
18.0	.643	.600	.536	.492	.455	.397	.399	.343	.312
21.5	.599	.575	.502	.487	.419	.380	.380	.322	.312
26.0	.536	.521	.477	.438	.414	.380	.341	.324	.278
30.0	.485	.473	.453	.421	.395	.367	.317	.302	.268
33.3	.585	.516	.444	.414	.382	.365	.341	.311	.309

AREA 4 (HALF SYMMETRY)

3.67	.371	.329	.310	.306	.312	.295	.299	.271	.276
6.0	.410	.373	.355	.340	.298	.293	.289	.310	.284
9.5	.418	.398	.377	.370	.358	.338	.355	.325	.333
14.0	.429	.409	.417	.400	.385	.386	.371	.363	.340
18.0	.480	.440	.412	.390	.389	.351	.362	.347	.329
21.5	.452	.437	.403	.407	.366	.351	.353	.329	.332
26.0	.456	.437	.418	.396	.386	.367	.344	.330	.317
30.0	.448	.429	.418	.407	.400	.388	.371	.345	.340
33.3	.476	.467	.416	.407	.403	.378	.384	.367	.377

CHAPTER 4

ANALYSIS OF DATA

The barrier factor depends upon the weight per unit area of the barrier, the type of material, the energy spectrum of the radiation and the angular distribution of the radiation striking the barrier. Spencer[5] has made extensive calculations involving the use of the Moments Method to determine the attenuation introduced by a vertical barrier adjacent to a horizontal field of contamination. The series of experimental measurements described in this report have been made (1) to test the validity of calculated barrier factors, and (2) to develop experimentally valid barrier factors for limited strips of contamination.

4.1 THE EXPERIMENT AS AN APPROXIMATION TO THE COMPUTED VALUES OF BARRIER FACTOR

The theoretical computation of barrier factor is based on an idealized geometry that may only be approximated during actual testing. It is thus necessary to estimate the effects of these approximations in order that the experimentally obtained data may be compared with that predicted by analytical means. The principle approximations are: (1) the experimental field, while flat in nature, is not a smooth plane in the mathematical sense, as in the theoretical case, and (2) the simulated field of contamination is not infinite in extent.

If the interface between earth and air is a rough rather than a smooth surface, a reduction in intensity is to be expected at lower detector positions. One method of treating ground irregularities (roughness, rolling effect) assumes that the source can be considered to be buried beneath a layer of soil in an infinite smooth plane, the depth of the hypothetical layer of soil depending upon the roughness of the ground. The reduction in dose rate due to the ground roughness is then considered to be equivalent to the number of mean free paths of soil overlaying the source. Experimental information necessary to check the accuracy of this method has been difficult to obtain, however, because of the difficulties in simulating and describing roughness in a meaningful way.

However, an estimate of the effect of ground roughness is

required if the data obtained are to be interpreted in a realistic way. Such an estimate was obtained experimentally by investigating the effects of ground roughness on the output of the test field. This experiment is described in detail in Reference 1. In brief, the experiment consisted of measuring the dose rate (in the absence of a test structure) at altitudes ranging from 1 to 33 feet above an "infinite" contaminated field and the comparison of these results with those theoretically computed. The experimentally measured dose rate for an infinite plane source, computed from the fields simulated in this experiment, are shown in Figure 4.1, together with a theoretical curve based upon the work of Spencer.[5] Comparison of the two indicates that the measured dose rate agrees with the theoretical values (within experimental accuracy) for detector heights above about 6 feet. The discrepancy at lower altitudes is attributed to deviations of the terrain from flatness. If the terrain deviates from mathematical flatness the lower detectors are shadowed by the raised portions of the field for sources of contamination located at a large distance from the detector. A "multiplicative factor" to correct experimentally obtained dose values for ground roughness was then determined by taking the ratio of the theoretical to experimental dose rates. The resulting multiplicative factors as a function of height are shown in Table 4.1.

The second approximation of the experiment to the theoretical situation lies in the fact that it is impossible to simulate an infinite field of contamination. Previous experiments, however, have indicated that a field extending to about ten times the structure height or one mean free path radius whichever is greater, is sufficient to provide most of the dose that would have been received from a truly infinite field. An analytical experimental procedure has been developed to estimate the attenuation afforded by a structure to radiation originating beyond the outermost experimental area. The basis for this procedure is that the angular distribution of radiation striking a vertical wall from sources at extremely large distances from the wall is not much different than that obtained from a contaminated field whose radius is greater than ten times the wall height. Thus the attenuation afforded by the structure to radiation from either far field contamination or the outermost simulated field is virtually identical. A detailed explanation of this calculation is presented in Reference 1.

If this estimate is expressed in mathematical form (See Figure 4.2), the dose arising from sources of contamination lying in the area extending

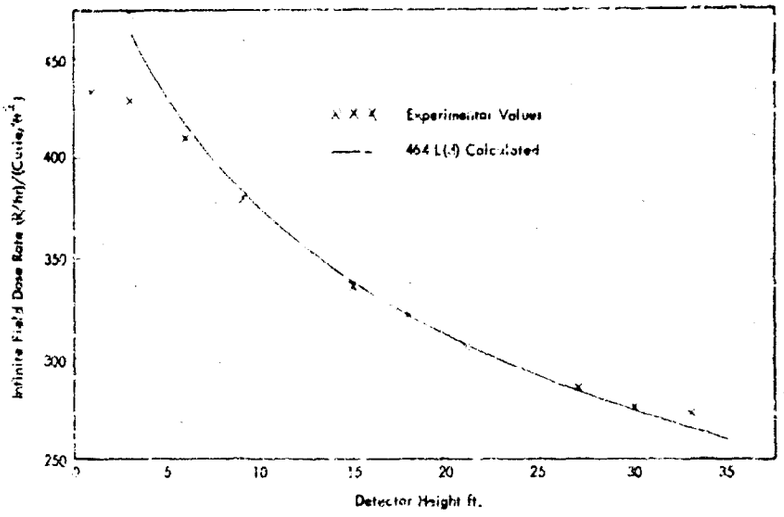

Figure 4. 1 - The Experimental and Theoretical Variation of Infinite Field Dose Rate with Altitude

TABLE 4. 1

INFINITE FIELD GROUND ROUGHNESS MULTIPLICATIVE FACTORS

DETECTOR HEIGHT (Feet)	MULTIPLICATIVE FACTOR
3.6	1.08
6.0	1.02
9.6	1.01
14	1.00
18	1.00
21.5	1.00
26	1.00
30	1.00
33.3	1.00

from radius r_o to infinity to that arising from contamination existing in the area bounded by r_i, r_o is

$$\text{Ratio} = \frac{D(h, r_o \quad \infty)}{D(h, r_i \quad r_o)} = \frac{E_1(\mu\rho_o) + 0.55e^{-\mu\rho_o}}{E_1(\mu\rho_i) - E_1(\mu\rho_o) + 0.55(e^{-\mu\rho_i} - e^{-\mu\rho_o})}$$

where

E_1 = exponential integral of the first kind

h = detector height

r_i, r_o = radii (see Figure 4.2)

$\rho_i \rho_o$ = slant radii (see Figure 4.2)

This equation has been evaluated for the experiment under discussion and is tabulated in Table 4.2 as a function of height. (See Appendix I for an estimate of the accuracy of this procedure).

4.2 COMPARISON OF EXPERIMENTAL AND THEORETICAL DATA

Measurements of the dose rate behind the exposed wall of the test structure were made at nine different heights at nine horizontal positions. Detector positions were symmetrically located with respect to the simulated contaminated area (as described in Chapter 3), and the readings of these symmetrically located detectors were combined to achieve results equivalent to contamination of the entire field external to the test wall. This combination of readings of symmetrically located detectors results in five distinct values of dose rate for each detector height for each area of contamination simulated. The values at each location must then be summed for each contaminated area and an estimate of the effects of "far field" sources of contamination added to achieve infinite field representation. Summation for each wall thickness are presented in Tables 4.3 through 4.7. There thus exist five experimental values of infinite field dose rate for each height, and, since these five values show excellent agreement, within normal experimental error, the

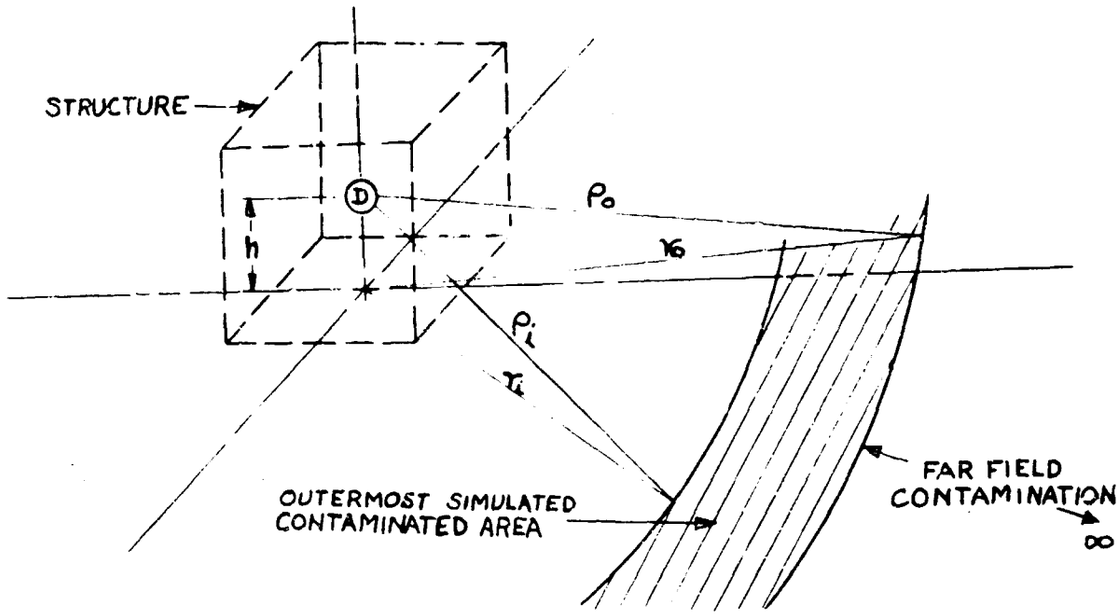

Figure 4.2 - Schematic Representation of Far Field Geometry

TABLE 4.2

RATIO OF "FAR FIELD" DOSE TO THAT OBTAINED FROM FURTHEST EXPERIMENTAL AREA SIMULATED

Detector Height (ft.)	Ratio	Detector h t (ft.)	Ratio
3.6	0.568	21.5	0.574
6.0	0.569	26	0.576
9.6	0.570	30	0.577
14.0	0.572	33.3	0.578
18.0	0.573		

average values may be used for purposes of comparison with theory. See Table 3.1 and Figure 3.2 for the dosimeter positions.

TABLE 4.3

Dose Rate Behind a Wall of Zero p.s.f. Thickness
$(R/hr)/(Curie/ft^2)$
(See Figure 3.2)

H = 3.6' (height)

POSITION	AREA 1	AREA 2	AREA 3	AREA 4	FAR FIELD	TOTAL
A	79.3	56.8	45.7	32.9	18.7	233.4
B	83.3	51.4	44.9	32.2	18.3	230.1
C	85.6	50.3	42.9	32.7	18.6	230.1
D	88.5	49.5	43.6	32.1	18.2	231.9
E	93.4	48.2	43.6	32.0	18.2	235.4
					Ave.	232.2

H = 6.0'

POSITION	AREA 1	AREA 2	AREA 3	AREA 4	FAR FIELD	TOTAL
A	57.9	57.8	46.2	35.8	20.4	218.1
B	62.2	50.8	44.6	35.1	20.0	212.7
C	64.6	50.1	44.6	35.8	20.4	215.5
D	67.5	48.3	44.6	34.1	19.4	213.9
E	67.0	48.2	44.9	34.8	19.8	214.7
					Ave.	215.0

H = 9.6'

POSITION	AREA 1	AREA 2	AREA 3	AREA 4	FAR FIELD	TOTAL
A	39.6	52.2	47.4	36.1	21.7	199.0
B	42.2	49.9	45.8	37.3	21.3	196.5
C		48.5	45.8	37.3	21.3	
D	47.1	46.9	45.1	37.5	21.4	198.0
E	46.8	46.8	45.8	36.8	21.0	197.2
					Ave.	197.7

H = 14.0'

POSITION	AREA 1	AREA 2	AREA 3	AREA 4	FAR FIELD	TOTAL
A	25.7	47.9	47.2	39.6	22.6	183.0
B	28.1	45.0	46.3	38.7	22.1	180.2
C	30.4	45.2	46.7	39.1	22.4	183.8
D	31.1	44.4	47.2	38.1	21.8	182.6
E	32.2	44.2	46.2	38.4	21.9	182.9
					Ave.	182.5

H = 18.0'

POSITION	AREA 1	AREA 2	AREA 3	AREA 4	FAR FIELD	TOTAL
A	19.1	42.4	46.8	40.7	23.3	172.3
B	20.5	40.7	46.2	38.9	22.3	168.6
C	22.1	40.2	45.8	39.6	22.7	170.4
D	23.7	39.5	45.5	39.1	22.4	170.2
E	24.4	40.3	45.6	39.2	22.5	170.0
					Ave.	170.7

H = 21.5'

POSITION	AREA 1	AREA 2	AREA 3	AREA 4	FAR FIELD	TOTAL
A	15.6	37.8	47.0	40.7	23.4	164.5
B	15.3	37.8	44.9	39.6	22.7	160.3
C	17.4	37.5	45.8	39.9	22.9	163.5
D	17.2	36.7	45.6	38.9	22.3	160.7
E	18.4	36.4	45.3	38.8	22.3	161.2
					Ave.	162.1

H = 26.0'

POSITION	AREA 1	AREA 2	AREA 3	AREA 4	FAR FIELD	TOTAL
A	11.1	34.6	45.6	40.9	23.5	155.7
B	11.8	33.0	44.2	39.6	22.8	151.4
C	12.2	34.3	44.3	39.4	22.7	152.9
D	12.1	33.7	45.3	39.6	22.8	149.7
E	12.8	34.7	45.3	39.4	22.7	152.9
					Ave.	152.5

H = 30.0'

POSITION	AREA 1	AREA 2	AREA 3	AREA 4	FAR FIELD	TOTAL
A	9.1	30.7	44.8	40.9	23.6	149.1
B	9.4	29.3	44.4	40.2	23.2	146.5
C	9.9	29.8	44.1	39.6	22.8	146.4
D	9.9	29.2	43.7	40.2	23.0	146.2
E	9.7	29.1	43.6	39.7	22.9	145.0
					Ave.	146.6

H = 33.3'

POSITION	AREA 1	AREA 2	AREA 3	AREA 4	FAR FIELD	TOTAL
A	7.6	29.1	44.4	41.4	23.9	144.4
B	7.8	26.6	41.5	40.5	23.4	139.8
C	8.2	27.1	43.4	39.7	23.2	141.6
D	8.4	26.4	42.8	39.9	23.1	140.6
E	8.5	27.6	43.1	39.7	22.9	139.8
					Ave.	141.4

TABLE 4.4

Dose Rate Behind a Wall of 49 p.s.f. Thickness
(R/hr)/(Curie/ft^2)
(See Figure 3.2)

H = 3.6' (height)

POSITION	AREA 1	AREA 2	AREA 3	AREA 4	FAR FIELD	TOTAL
A	14.6	15.9	11.6	7.9	4.5	54.5
B	16.3	14.9	12.1	8.0	4.5	55.8
C	16.3	13.3	11.3	7.6	4.3	52.8
D	16.4	12.4	11.1	7.4	4.2	51.5
E	19.7	14.0	12.4	8.3	4.7	59.1
					Ave.	54.7

H = 6.0'

POSITION	AREA 1	AREA 2	AREA 3	AREA 4	FAR FIELD	TOTAL
A	8.4	14.5	12.2	8.4	4.8	48.3
B	9.9	13.5	12.1	3.8	5.0	49.3
C	10.8	13.1	12.0	8.5	4.8	49.2
D	10.7	12.0	11.8	8.4	4.8	47.7
E	10.5	11.8	11.0	7.8	4.4	45.6
					Ave.	48

H = 9.6'

POSITION	AREA 1	AREA 2	AREA 3	AREA 4	FAR FIELD	TOTAL
A	5.2	12.5	12.3	9.2	5.2	44.4
B	5.8	12.4	12.2	9.2	5.2	44.8
C	6.6	12.2	12.4	9.5	5.4	46.1
D	6.7	12.1	12.1	9.2	5.2	45.3
E	6.7	11.5	11.8	9.8	5.0	43.8
					Ave.	44.9

H = 14'

POSITION	AREA 1	AREA 2	AREA 3	AREA 4	FAR FIELD	TOTAL
A	2.7	10.2	11.8	9.3	5.3	39.3
B	3.4	10.8	12.3	9.7	5.5	41.7
C	3.5	10.4	12.4	9.8	5.6	41.7
D	3.6	10.5	12.0	9.7	5.5	41.3
E	3.8	10.0	11.8	9.6	5.5	40.7
					Ave.	40.9

H = 18'

POSITION	AREA 1	AREA 2	AREA 3	AREA 4	FAR FIELD	TOTAL
A	1.5	8.8	12.1	10.0	5.7	38.1
B	1.9	9.0	11.8	9.8	5.6	38.1
C	2.1	8.5	11.8	9.8	5.6	37.8
D	2.1	8.4	11.2	9.2	5.3	36.2
E	2.2	8.6	11.8	9.7	5.6	37.9
					Ave.	37.6

H = 21.5'

POSITION	AREA 1	AREA 2	AREA 3	AREA 4	FAR FIELD	TOTAL
A	0.93	6.9	11.2	--		
B	1.2	7.6	11.4	9.9	5.7	35.8
C	1.2	7.4	11.6	9.6	5.5	35.8
D	1.4	7.1	11.1	9.3	5.3	34.2
E	1.5	7.4	11.2	9.6	5.5	35.2
					Ave.	35.3

H = 26'

POSITION	AREA 1	AREA 2	AREA 3	AREA 4	FAR FIELD	TOTAL
A	0.57	5.92	11.3	9.7	5.6	33.1
B	0.74	5.88	10.9	9.9	5.7	33.1
C	0.71	5.56	10.7	9.5	5.5	32.0
D	0.75	5.76	10.5	9.4	5.4	32.0
E	0.84	6.04	11.0	9.6	5.6	33.0
					Ave.	32.6

H = 30'

POSITION	AREA 1	AREA 2	AREA 3	AREA 4	FAR FIELD	TOTAL
A	0.42	4.28	10.6	9.8	5.7	31.0
B	0.49	4.92	10.6	9.7	5.6	31.0
C	0.50	4.92	10.5	9.8	5.7	31.0
D	0.55	4.93	10.7	9.8	5.7	31.7
E	0.57	4.94	10.7	9.8	5.7	31.7
					Ave.	31.3

H = 33.3'

POSITION	AREA 1	AREA 2	AREA 3	AREA 4	FAR FIELD	TOTAL
A	0.34	4.55	10.8	10.5	6.1	32.3
B	0.35	4.45	10.6	9.9	5.7	31.0
C	0.37	4.51	10.4	9.8	5.7	31.0
D	0.40	4.18	9.9	9.8	5.7	30.0
E	0.38	4.08	10.6	9.9	5.7	31.0
					Ave.	31

TABLE 4.5

Dose Rate Behind a Wall of 90 p.s.f. Thickness
$(R/hr)/(Curie\ 1\ ft^2)$
(See Figure 3.2)

H = 3.6' (height)

POSITION	AREA 1	AREA 2	AREA 3	AREA 4	FAR FIELD	TOTAL
A	4.22	5.00	3.68	2.18	1.24	16.32
B	4.65	4.70	3.57	2.20	1.25	16.37
C	4.69	4.34	3.60	2.09	1.19	15.91
D	4.90	4.05	3.46	2.06	1.17	15.64
E	5.25	4.36	3.70	2.30	1.31	16.93
					Ave.	16.23

H = 6.0'

POSITION	AREA 1	AREA 2	AREA 3	AREA 4	FAR FIELD	TOTAL
A	2.30	4.29	3.68	2.44	1.39	14.10
B	2.79	4.26	4.01	2.45	1.39	14.90
C	2.76	3.64	3.47	2.32	1.32	13.51
D	2.79	3.59	3.46	2.32	1.32	13.48
E	2.78	3.58	3.30	2.26	1.28	13.20
					Ave.	13.84

H = 9.5'

POSITION	AREA 1	AREA 2	AREA 3	AREA 4	FAR FIELD	TOTAL
A	1.21	3.90	3.72	2.63	1.49	12.95
B	1.38	3.74	3.51	2.61	1.48	12.72
C	1.42	3.61	4.48	2.64	1.50	13.65
D	1.62	3.43	3.53	2.59	1.47	12.57
E	1.56	3.36	3.44	2.52	1.43	12.31
					Ave.	12.90

H = 14.0'

POSITION	AREA 1	AREA 2	AREA 3	AREA 4	FAR FIELD	TOTAL
A	.49	2.70	3.46	2.64	1.51	10.80
B	.63	2.80	3.67	2.69	1.54	11.33
C	.68	2.90	3.60	2.65	1.52	11.35
D	.70	2.83	3.46	2.69	1.54	11.22
E	.74	2.88	3.56	2.70	1.54	11.42
					Ave.	11.32

H = 18.0'

POSITION	AREA 1	AREA 2	AREA 3	AREA 4	FAR FIELD	TOTAL
A	.27	2.32	3.62	2.88	1.65	10.74
B	.35	2.31	3.53	2.79	1.60	10.58
C	.35	2.26	3.40	2.78	1.59	10.38
D	.37	2.20	3.39	2.66	1.52	10.14
E	.40	2.40	3.50	2.76	1.58	10.64
					Ave.	10.50

H = 21.5'

POSITION	AREA 1	AREA 2	AREA 3	AREA 4	FAR FIELD	TOTAL
A	.16	1.83	3.25	2.66	1.53	9.43
B	.20	1.93	3.39	2.66	1.53	9.71
C	.22	1.93	3.15	2.63	1.51	9.44
D	.24	2.00	3.25	2.68	1.54	9.71
E	.24	1.94	3.16	2.55	1.46	9.35
					Ave.	9.53

H = 26'

POSITION	AREA 1	AREA 2	AREA 3	AREA 4	FAR FIELD	TOTAL
A	.096	1.36	3.19	2.72	1.57	8.87
B	.11	1.45	3.02	2.72	1.57	8.87
C	.12	1.42	3.15	2.70	1.56	8.95
D	.12	1.37	3.05	2.67	1.54	8.75
E	.14	1.50	3.2[illegible]	2.70	1.[illegible]	9.12
					Ave.	8.91

H = 30'

POSITION	AREA 1	AREA 2	AREA 3	AREA 4	FAR FIELD	TOTAL
A	0.060	1.06	2.88	2.80	1.62	8.42
B	0.072	1.16	3.01	2.72	1.57	8.53
C	0.076	1.13	3.02	2.73	1.58	8.55
D	0.084	1.17	3.01	2.78	1.60	8.64
E	0.088	1.22	3.16	2.80	1.62	9.04
					Ave.	8.61

H = 33.3'

POSITION	AREA 1	AREA 2	AREA 3	AREA 4	FAR FIELD	TOTAL
A	.051	1.09	3.33	2.87	1.72	9.16
B	.055	1.04	3.13	2.78	1.65	8.64
C	.054	1.03	2.95	2.81	1.62	8.46
D	.056	1.03	2.91	2.81	1.66	8.51
	.056	1.06	3.02	2.[illegible]	1.[illegible]	8.[illegible]
					Ave.	8.[illegible]

TABLE 4.6

Dose Rate Behind a Wall of 147 p.s.f. Thickness
(R/hr)/(Curie 1 ft^2)
(See Figure 3.2)

H = 3.6' (height)

POSITION	AREA 1	AREA 2	AREA 3	AREA 4	FAR FIELD	TOTAL
A	1.15	1.47	1.07	0.65	0.37	[illegible]
B	1.29	1.30	1.01	0.60	0.34	4.54
C	1.21	1.23	0.96	0.61	0.35	4.36
D	1.49	1.20	0.97	0.60	0.34	4.60
E	1.37	1.20	1.05	0.62	0.35	4.59
					Ave.	4.49

H = 6.0'

POSITION	AREA 1	AREA 2	AREA 3	AREA 4	FAR FIELD	TOTAL
A	0.55	1.32	1.04	0.69	0.39	3.99
B	0.63	1.19	1.00	0.68	0.39	3.89
C	0.64	1.08	0.94	0.64	0.36	3.66
D	0.66	1.01	0.93	0.63	0.36	3.59
E	0.64	0.94	0.88	0.60	0.34	3.40
					Ave.	3.71

H = 9.6'

POSITION	AREA 1	AREA 2	AREA 3	AREA 4	FAR FIELD	TOTAL
A	0.26	1.07	1.03	0.75	0.43	3.54
B	0.31	0.97	0.99	0.72	0.41	3.40
C	0.34	0.99	1.00	0.73	0.42	3.48
D	0.36	0.94	0.97	0.71	0.40	3.38
E	0.37	0.92	0.96	0.72	0.41	3.38
					Ave.	3.44

H = 14.0'

POSITION	AREA 1	AREA 2	AREA 3	AREA 4	FAR FIELD	TOTAL
A	.095	.739	.958	.769	.439	3.00
B	.121	.749	.971	.762	.436	3.04
C	.136	.743	.974	.768	.439	3.06
D	.141	.738	.977	.785	.449	3.08
E	.148	.730	.960	.770	.440	3.05
					Ave.	3.04

H = 18'

POSITION	AREA 1	AREA 2	AREA 3	AREA 4	FAR FIELD	TOTAL
A	.052	.535	.955	.805	.461	2.81
B	.062	.603	.943	.787	.451	2.85
C	.068	.578	.935	.774	.443	2.80
D	.070	.564	.889	.741	.424	2.69
E	.079	.590	.910	.778	.446	2.80
					Ave.	2.79

H = 21.5'

POSITION	AREA 1	AREA 2	AREA 3	AREA 4	FAR FIELD	TOTAL
A	.030	.499	.911	.784	.450	2.67
B	.036	.496	.897	.762	.437	2.63
C	.039	.497	.882	.756	.434	2.61
D	.042	.480	.867	.758	.435	2.58
E	.040	.500	.838	.732	.420	2.53
					Ave.	2.60

H = 26

POSITION	AREA 1	AREA 2	AREA 3	AREA 4	FAR FIELD	TOTAL
A	.015	.319	.814	.769	.443	2.36
B	.020	.352	[illegible]	.787	[illegible]	2.46
C	.022	.342	.818	.762	.439	2.38
D	.023	[illegible]	.818	[illegible]	.439	2.38
E	.026	.362	.828	[illegible]	.443	2.43
					Ave.	[illegible]

H = 30.0

POSITION	AREA 1	AREA 2	AREA 3	AREA 4	FAR FIELD	TOTAL
A	[illegible]	[illegible]	[illegible]	.780	[illegible]	2.23
B	.013	[illegible]	[illegible]	.774	.446	2.27
C	.014	[illegible]	[illegible]	.769	.444	2.27
D	[illegible]	[illegible]	[illegible]	[illegible]	.459	2.33
E	[illegible]	[illegible]	[illegible]	[illegible]	.462	2.34
					Ave.	[illegible]

H [illegible]

POSITION	AREA 1	AREA 2	AREA 3	AREA 4	FAR FIELD	TOTAL
A	[illegible]	[illegible]	[illegible]	[illegible]	[illegible]	[illegible]
B	[illegible]	[illegible]	[illegible]	[illegible]	[illegible]	[illegible]
C	[illegible]	[illegible]	[illegible]	[illegible]	[illegible]	[illegible]
D	[illegible]	[illegible]	[illegible]	[illegible]	[illegible]	[illegible]
E	[illegible]	[illegible]	.244	[illegible]	[illegible]	[illegible]
					Ave.	[illegible]

Spencer[5] has calculated the dose rate that would be measured by a detector located behind a vertical wall, subjected to a semi-infinite field of contamination (as in this experiment) extending from the base of the wall to an infinite radius for both cobalt and fallout radiation. The function $W(x, d)$ defined by Spencer is equivalent to one-half of the dose rate that would be received by a detector located between two infinitely high and wide walls due to a semi-infinite source field located on each side. While a direct comparison between $W(x, d)$ and the experimental data may be made, the vertical wall barrier factor, $B(x_e, h)$, is the parameter that we wish ultimately to evaluate. This parameter is referred to in "Engineering Manual Style Calculations",[2, 3, 4, 5] and is numerically equal to twice the function $W(x, d)$.

Table 4.7 and Figure 4.3 summarize the average values of the experimentally measured dose rates of Tables 4.3 through 4.6 normalized to the source density that would produce one R/hr at a 3 foot detector height, if the field were infinite in extent, and presents the theoretical values of $W(x, d)$ for cobalt radiation thereby permitting a direct comparison.

The experimental values shown in Table 4.7 agree very well with the calculated values for dose variation with height. However, while the experimental reduction factors are in excellent agreement with theory for the 0 psf barrier, discrepancies of 12, 18 and 24 per cent exist for the 49, 98 and 147 psf barriers respectively. The experimental results are lower in all cases. It is of interest to note that the experimental barrier factors are equivalent to attenuation provided by calculated barrier factors of 53, 106 and 159 pst walls, as illustrated in Figure 4.4. Thus the experimentally measured barrier factor is equivalent to that calculated theoretically for a mass thickness of 108 percent of actual thickness in each instance. This result, as it is proportional to wall mass thickness, might be attributed to errors in either the cross section of the barrier or the energy spectrum of the incident radiation. The detailed method of calculation used to generate the theoretical estimates of $W(x, d)$ assumed that the spectrum incident on the wall was the same as the source spectrum rather than that actually existing at the wall-air interface. This assumption was expected to produce values of barrier attenuation that were conservative in nature. That this actually occurs is thus confirmed by the experiment.

The discrepancies noted above between theoretical and experimental results are of the order of 12, 18 and 24 percent. This difference

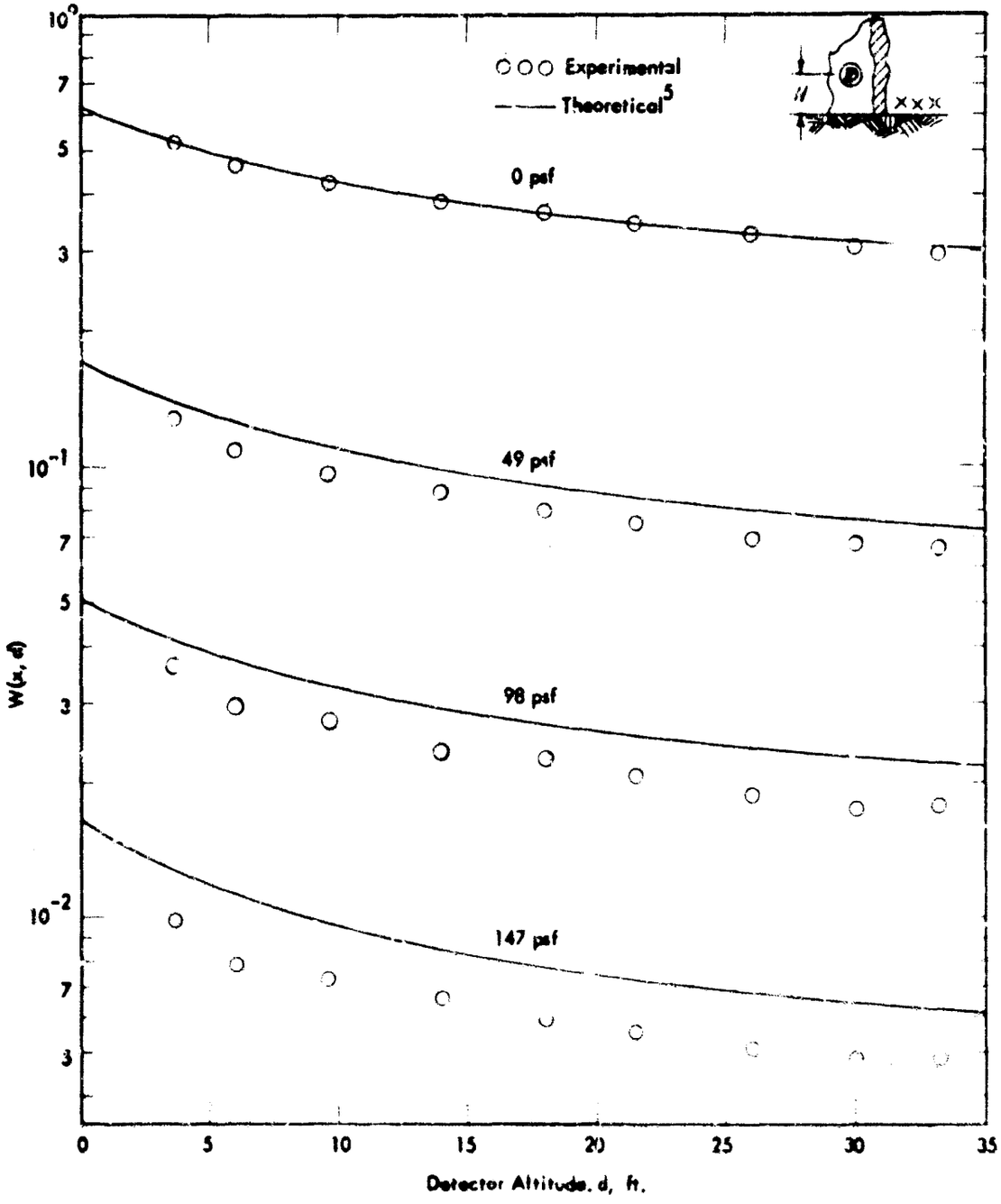

Figure 4.3 - The Barrier Factor W(x, d) for Cobalt Radiation

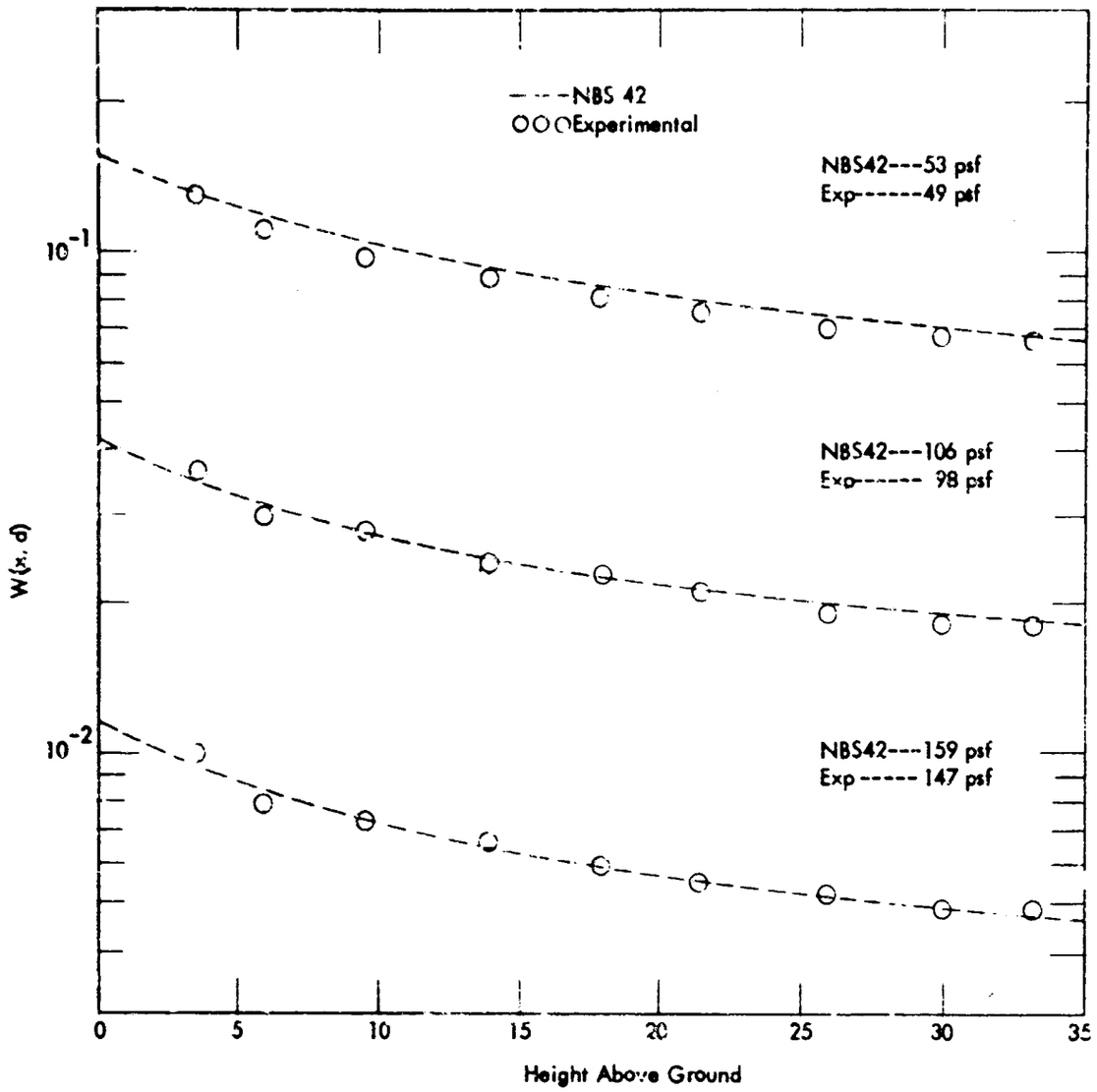

Figure 4.4 - Experimental Attenuation for a Given Thickness Compared with that Calculated for 108 percent of that Thickness

TABLE 4.7

BARRIER ATTENUATION FACTOR W(x, d) FOR COBALT RADIATION

W(x, d)

Height Above Ground	X = 0 psf		X = 49 psf		X = 98 psf		X = 147 psf	
	EXP.	NBS 42	EXP.	NBS 42	EXP.	NBS 42	EXP.	NPS 42
3.6	.53	.53	.13	.14	.037	.042	.010	.013
6.0	.47	.48	.11	.13	.030	.038	.008	.011
9.6	.43	.43	.098	.11	.028	.033	.0074	.0098
14	.39	.39	.089	.10	.024	.030	.0067	.0086
18	.37	.37	.081	.093	.023	.027	.0060	.0079
21.5	.35	.35	.076	.087	.021	.026	.0056	.0074
26	.33	.33	.070	.082	.019	.025	.0052	.0069
30	.31	.32	.068	.077	.018	.023	.0049	.0065
33.3	.30	.31	.067	.074	.018	.022	.0049	.0063

is sufficiently above the expected experimental error of slightly under ± 3% (See Section 3.1 and Appendix A) that it may be concluded that the present methods of calculation are conservative.

4.3 FINITE FIELD BARRIER FACTORS

In the calculation of the shelter afforded by structures from fallout gamma radiation, interest is often directed toward structures subjected to finite fields of contamination. The Engineering Manual method[2] of computing the dose expected from finite sources of radiation in the center of a structure is based on a simple correction to the infinite plane results.

The basic assumption made in treating finite sources is that non-wall-scattered and wall-scattered radiation must be treated differently. Non-wall-scattered radiation in a structure depends on the solid

angle (ω_ℓ) subtended by the source area, at the detector position, since it is composed mainly of radiation which travels directly from source to detector. In the case of wall-scattered radiation, however, the wall acts as a secondary source. The amount of radiation impinging on the wall is a function of the solid angle fraction subtended at the center of the wall by the source area. The radiation scattered in the wall and reaching the detector depends on the solid angle of the wall as viewed by the detector, thus the wall-scattered radiation depends on two solid angles.

In calculating the non-wall-scattered radiation from a finite source the geometry factor, which is obtained by differentiating between the response for the outer dimensions of the source area and the response for the inner dimensions, is multiplied by the barrier factor for the infinite plane source:

$$C_g = \left[G_d(\omega'_\ell, H) - G_d(\omega''_\ell, H)\right] \left[1 - S_w(x_e)\right] B_e(x_e, H)$$

where ω'_ℓ is the solid angle fraction subtended at the detector by the inner dimensions of the structure and ω''_ℓ is the solid angle fraction subtended by the outer dimensions of the contaminated area.

In calculating the contribution from wall-scattered radiation, the G_s curve is used for the geometry factor in the case of limited fields since the geometry factor for wall scattered radiation is assumed to be independent of the source geometry because of multiple scattering in the wall. The geometry factor for wall-scattered radiation thus must be multiplied by a barrier factor for finite sources to account for the finiteness of the contaminated area.

$$G_g = \left[G_s(\omega_\ell) + G_s(\omega_u)\right] S_w(x_e) B_{ws}(\omega_s, x_e)$$

The barrier factor $B_{ws}(\omega_s, x_e)$ for finite sources is based on unpublished calculations of Spencer, in which he calculated the dose rate behind a wall due to direct radiation from semicircular sources. These semicircles were concentric about a point at the base of the wall directly below the center of the wall. The results are a function of the wall thickness and the solid angle fraction $\omega_s/2$ subtended by the source.

It should be noted he e that the curves $B_{ws}(\omega_s, x_e)$ which appear in Chart 9 of the Engineering Manual and are designated as barrier reduction factors for wall-scattered radiation for Limited Strips of Contamination, are in actuality Spencer's data which includes both wall-scattered and non-wall-scattered radiation. The designation given in the Engineering Manual refers to their use rather than the make up, i.e., to be used only in calculating wall-scattered radiation contribution.

The experiment described in this report involved the simulation of an infinite field of contamination by combining results obtained from circular contaminated annular areas and thus affords an opportunity to evaluate the effects of finite fields of contamination. Unfortunate', the theoretical estimates of this effect have only been computed for the fallout energy spectrum while the experiment was performed using Cobalt-60. However, the relative effects of field size are expected to be quite similar in both cases.

In order to compare the experimentally obtained results with those calculated from theory, it was necessary to calculate the solid angle fraction subtended by the source area at the detector location at the middle of the experimental wall in the horizontal direction. As was stated in Chapter 3, the simulated contaminated areas consisted of quarter circular sectors, whose centers coincided with the center of the test structure rather than the foot of the wall. The contaminated area as viewed by the detector at the center of the wall is as shown in Figure 4.5. The solid angle fraction subtended by this area as viewed by the detector is estimated as approximately equal to the average of the solid angle fractions of the two circles defined by minimum and maximum radii. The solid angle fraction ω, therefore, as illustrated in Figure 4.5 is;

$$\omega = 1 - \left[\frac{\dfrac{h}{\sqrt{h^2 + r_w^2}} + \dfrac{h}{\sqrt{h^2 + r_o}}}{2} \right]$$

where:

h = detector height above ground

r_o = maximum radius of contaminated area as measured from the center of wall

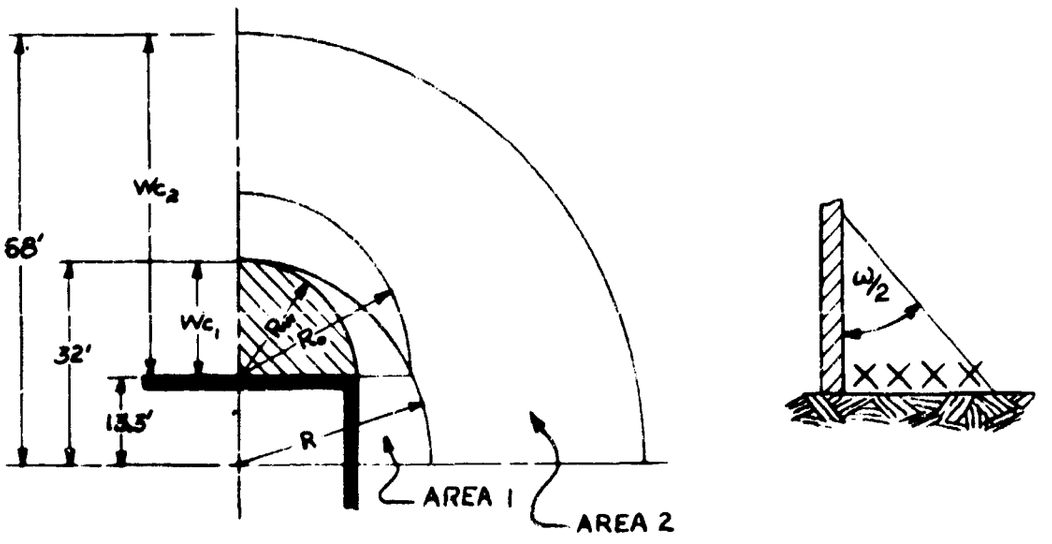

Figure 4.5 - Approximation of Solid Angle Fraction

r_w = minimum radius of the contaminated area measured from the center of wall

Unlike the infinite field results, only data obtained at the center of the wall (Position E) (See Figure 3.2) may be used to determine the reduction factors for limited fields. (Only Position E is centered relative to the field for small field radii). The normalized data for this position are plotted in cumulative form in Figure 4.6 as a function of solid angle for all barrier mass thicknesses investigated. The dashed line shown in this figure represents computed values based upon the fallout energy spectrum. While a direct comparison cannot be made between theoretical values based on fallout radiation and those experimentally measured using Cobalt-60 radiation, some indication of the relative agreement is possible. It is clear from Figure 4.6 that the relative agreement is excellent for small fields of contamination, while for larger fields of contamination, experimental values tend to increase at a somewhat slower rate, causing the experimental curves to become much flatter. The effect of air attenuation is clearly evident for

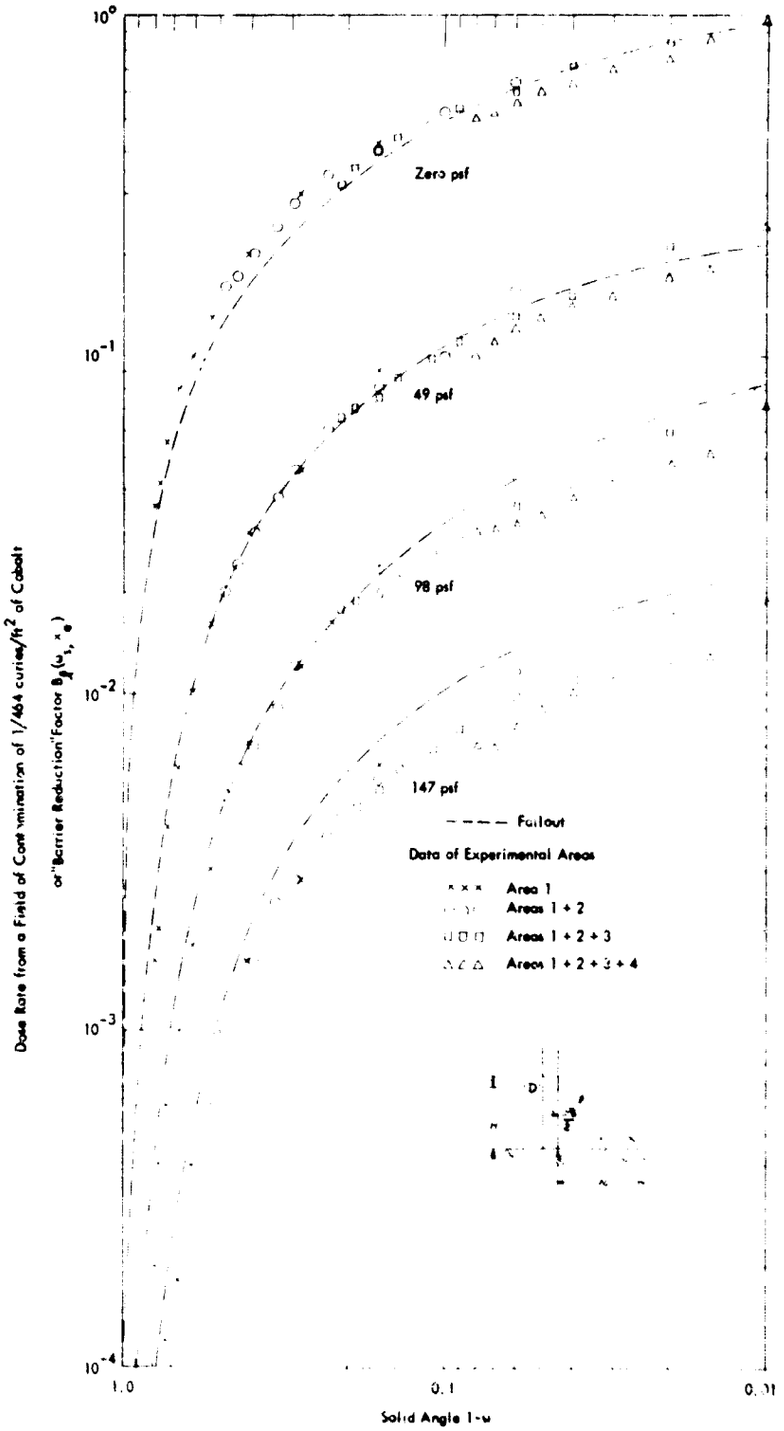

Figure 4.6 – The Effect of Limited "Circular" Fields of Contamination

detector positions of different heights for which the field subtends the same solid angle fraction. This condition occurred at several positions on the curve, most notably where $1-\omega = .05$ and $.16$. Here it can be seen that the barrier factor $B_w(x_e, \omega_s)$, decreases with height for the same solid angle. Note that $B_\omega(x_e, \omega_s)$ is not a function of height and hence breaks down at large heights and consequently large air attenuation. Agreement between calculated fallout results and experimental Cobalt values is very good for the 0 and 49 psf cases, as might be expected since the penetration data for fallout and Cobalt radiation are, for all practical purposes, identical for concrete mass thicknesses below 80 psf.

CHAPTER 5

CONCLUSIONS AND RECOMMENDATIONS

5.1 GENERAL

The purpose of this experiment has been to evaluate the attenuation of ground based sources of radiation by a vertical slab so that the effect of this attenuation may be removed from later experiments designed for the measurement of other shelter parameters. To accomplish this task four series of experimental measurements were undertaken. All of these series were identical except that the wall thickness was varied from 0, to 49, to 98 to 147 psf. Each test series was comprised of the determination of barrier attenuation as a function of detector height and size of the contaminated field.

5.2 CONCLUSIONS

The major conclusions that can be drawn from this work may be summarized as follows:

1. The agreement of variation of wall barrier factor, $\frac{B(x_e, h)}{B(x_e, h = 3)}$ with height for all mass thicknesses with that predicted theoretically is excellent.

2. The experimental value of barrier factor is found to be approximately equal to the theoretical value for 108% of actual wall thickness in all cases tested. The theoretical values presently used in shelter calculations are thus conservative.

3. The variation of wall attenuation with size of the contaminated field, while not directly comparable with any existing theoretical estimates, is similar to that predicted for the spectra of 1.12 hr. fallout, particularly for walls of less than 80 psf thickness.

5.3 RECOMMENDATIONS

The major recommendations resulting from this study are that,

1. The theoretical values of the barrier attenuation factors for vertical walls that are presently used, be continued as representing a conservative estimate of actual attenuation.

2. Further experimental work be undertaken to evaluate the effect of limited rectangular as well as circular strips of contamination.

3. Theoretical estimates of the dose rate from limited circular strips of cobalt contamination be undertaken to correlate with the experimental data presented.

REFERENCES

1. "Description, Experimental Calibration and Analysis of the Radiation Test Facility at the Protective Structures Development Center", C. A. McDonnell, J. Velletri, A. W. Starbird, J. F. Batter, P. S. D. C. TR-14, Sept. 1964

2. "The Design and Review of Structures for Protection from Fallout Gamma Radiation, Office of Civil Defense, Professional Manual PM-100-1, February 1965

3. "Shelter Design and Analysis", Office of Civil Defense, Sept. 1962

4. "An Engineering Method for Calculating Protection Afforded by Structures Against Fallout Radiation", Office of Civil Defense OCD PM-100-1, Supplement No. 1, Charles Eisenhauer. January 1964

5. "Structural Shielding Against Fallout Radiation", L. V. Spencer, NBS Monograph 42

6. "Scattered Radiation and free Field Dose Rates from Distributed Cobalt-60 and Cesium 137 Sources", Ralph Rexroad and Murray Schmoke, NDL-TR-2, Sept. 1960

APPENDIX A

ERRORS ASSOCIATED WITH THE EXPERIMENTAL AND ANALYTICAL TECHNIQUES

It is of interest to determine the probable error associated with this experiment so that judgements may be made as to the validity of both the experimental data itself and the conclusionsdrawn from the analysis of this cata. For discussional purposes the sources of error in this experiment may be lumped into five basic categories. These are:

1. Instrumental errors (in dose measurement) caused by the various conditions of weather, exposure rate, source strength and exposure time encountered during the experiment.

2. Instrument errors associated with the minor variations of manufacturing tolerances encountered in the production of the large number of instruments used.

3. Measurement errors in the mass thickness of the items tested.

4. Systematic errors due to errors in basic calibrations, etc.

5. Extrapolation errors introduced by the estimation of far field results.

The error that is associated with the first three of these categories has been discussed in Section 3.1 of this report and in Reference 1. In these the standard deviation of instrument response under a wide variety of atmospheric conditions, dose rate and exposure time was measured. The standard deviation of any given instrument under all experimental conditions encountered was found to be 2.3% and the instrument to instrument variation less than 2 percent throughout all instruments used.

The standard deviation in test slab thicknesses, was found to be one percent. This one percent in mass thickness, corresponds to a standard deviation of from one to two percent in dose rate, depending upon the mass thickness. At higher mass thicknesses an error in the mass thickness corresponds to larger errors in the dose rate measured (See Reference 5).

Systematic errors, attributable to errors introduced during the calibration of sources or detectors, are not expected to be present in an experiment of this type because the data reported is all normalized to a condition measured with the same equipment, that of 464 (R/hr)/(curie/ft^2). Thus, even though the experimental data is reported as a dose rate or total accumulated dose, the actual normalization procedure requires that these quantities be ratios of previously measured values in the absence of the structure to be tested.

The major source of analytical error is that introduced by the extrapolation procedure used to estimate the effects of a field of contamination extending from the outermost radius of that simulated (452 ft) to infinity. To estimate the effect of this "missing" contamination two assumptions are made; first that the dose build-up factor, point source to point detector, near a ground air interface may be adequately represented by a polynomial expansion of the form $B(\mu\rho) = 1+0.55\ \mu\rho$, and secondly that the attenuation introduced by a vertical wall to the contamination existing beyond 452 feet radius is identical to that for a field of contamination existing from 164 to 452 foot radius. To evaluate the first of these assumptions we may estimate the amount of "far field radiation" using various methods of approximation. The fraction of the total dose rate above an infinite field represented by the contamination existing beyond 452 foot radius may be (1) determined from the experimental data of Rexroad, (2) computed using the results of the moments calculation of Spencer[5], (the dose rate above the center of a cleared circle is expressed by Spencer as $L(\rho)$ where ρ is the slant distance from the edge of the circle to the detector), and (3) computed by summing point source point detector values using $B(\mu\rho) = 1+0.55\ \mu\rho$ as the dose build-up factor as in the method of this report. The results of this manipulation for two altitudes typical of the minimum and maximum investigated in this study are illustrated in Table A-1. The estimate of far field contribution used in this report agrees somewhat better with the experiments of Rexroad[6] than with the calculation of Spencer. The reason for this may be attributed to the fact that Spencer's moment calculations were performed in an infinite medium neglecting the effect of the density interface. This lack of density interface affect is expected to over-emphasize the scattered dose contribution from the far field region.

The assumption that the attenuation of a vertical wall is identical for radiation arising from the area beyond 452 feet and from the annulus extending from 164 to 452 feet may be the more tenuous

TABLE A-1

Fraction of Infinite Field Dose Rate Attributable to Contamination Beyond 452 ft. Radius and the Ratio of that Dose Rate to that Attributable to the Region Extending from 164 to 452 ft/radius

Height	Fraction	Data of Reference	Ratio
3	.08	Rexroad[6]	0.56
3	.11	Spencer[5]	0.65
33	.19	Spencer[5]	0.65
3	.082	This report	0.57
33	.157	This report	0.58

of the two assumptions. This is because a larger portion of the total dose arising from contamination lying beyond 452 ft. radius would be caused by scattered radiation and thus be of softer energy spectrum than that arising from the annular area extending from 164 to 452 feet. The direct and scattered portion of the total dose attributable to each area may be calculated directly if the assumption as to build-up factor is allowed. The attenuation provided by the wall may, however, only be estimated crudely. The unscattered radiation is obviously that of the source energy, cobalt. Since this radiation originates at large distances from the structure, the radiation arrives approximately parallel to the ground. We may then use as an approximation of the attenuation of these gamma rays the attenuation computed for parallel monodirection gamma rays having an incident obliquity of zero degrees. Most of the scattered radiation that reaches the wall of the structure will also similarly arrive parallel to the ground but with a lower energy spectrum. If we assume that the energy of this radiation is near that of Cesium 137, we may then use as an approximation the attenuation values for parallel monodirectional gamma rays of incident obliquity of zero degrees for Cesium radiation. Data of this type is presented in Reference 5. Using these assumptions the dose rate behind the attenuating wall may then be calculated. The results of this calculation is presented in Table A-2 as the ratio of the dose attributable to radiation originating from sources lying beyond 452 feet radius to that arising from the 164 to 452 foot radius annulus

for various mass thicknesses and detector heights.

TABLE A-2

Far Field Dose as a Fraction of that Attributable to 164 to 452 ft. Annulus

Mass thickness (psf)	Detector altitude (ft.)	Fraction	% error attributable assuming zero mass case			
			As fraction of 164-452 ft this report	As fraction of infinite field dose		
				this report	Rexroad[6]	Spencer[5]
0	3	0.568	0%	--	--	--
0	33	0.578	0%	--	--	--
50	3	0.551	-3%	-0.25%	-0.25%	-0.33%
50	33	0.564	-2%	-0.31%	--	-0.38%
100	3	0.529	-7%	-0.57%	-0.56%	-0.77%
100	33	0.541	-6%	-0.94%	--	-1.10%
150	3	0.517	-9%	-0.74%	-0.72%	-0.99%
150	33	0.528	-9%	-1.41%	--	-1.71%

This table indicates that though the estimate of this far field dose (attributable to contamination existing beyond 452 ft. radius) within a structure of 150 psf thickness may be in error by as much as 9% of that originating from the 164-452 ft. annulus. This error represents significantly less than two percent of the total dose. The situation improves further as wall thickness decreases.

To summarize, the errors directly attributable to the experimental technique of this study are those of reproducibility, instrument accuracy, mass thickness determination, and systematic errors introduced by the technique. The standard deviation of each of these errors have been found to be about 2%. The probable error associated with all these sources of errors are thus;

$$P = \pm 0.6745 \sqrt{\sigma_1^2 + \sigma_2^2 + \sigma_3^2 + \sigma_4^2}$$

$$= \pm 2.2\% \text{ for zero psf}$$

$$= \pm 2.5\% \text{ for 150 psf}$$

Similarly, the error in total dose rate associated with assuming the attenuation of the vertical wall to be identical for radiation originating in both the far field region and the 164-452 ft. annulus is estimated as;

height thickness	3 ft.	33 ft.
0 psf	-0%	- 0%
50 psf	-0.3%	- 0.3%
100 psf	-0.6%	- 1.0%
150 psf	-0.8%	- 1.6%